

TOPICAL REVIEW

Compact Substrate Integrated Waveguide Filtering Antennas: A Review

XIAONAN SUN¹, JITONG MA¹, YULIN FENG¹, JUN SHI², (Member, IEEE),
AND ZHIXIA XU^{1,3}, (Member, IEEE)

¹School of Information Science and Technology, Dalian Maritime University, Dalian 116026, China

²Department of Electrical Engineering, California Institute of Technology, Pasadena, CA 91125, USA

³State Key Laboratory of Millimeter Waves, Southeast University, Nanjing 210096, China

Corresponding authors: Jitong Ma (majitong@dlnu.edu.cn), Jun Shi (shijun@caltech.edu), and Zhixia Xu (zxxu@163.com)

This work was supported in part by the National Natural Science Foundation of China under Grant 62101090, in part by the China Postdoctoral Science Foundation with under Grant 2021M700656, in part by the State Key Laboratory of Millimeter Waves under Grant K202202, and in part by the Fundamental Research Funds for the Central Universities under Grant 3132022240 and Grant 3132022229.


ABSTRACT In recent years, with the rapid development of integrated circuits, the filtering antenna (FA) circuit of the substrate integrated waveguide (SIW) has attracted widespread attention in wireless communications. Numerous structures have been proposed to improve the performance of SIW FA. Hence, this paper presents the development and miniaturization trend of the SIW FA, and briefly introduces the structure and historical development of the SIW FA. In terms of the mode, multi-mode cavities and incomplete mode cavities are constructed. Multi-layer structures, special structures and the slow-wave technology are constructed in physical structure. Several methods and design examples of the SIW FA miniaturization are introduced from these two aspects. Based on the combination of the filter and antenna, the FA remains the advantages of the SIW structure, mainly including small size, low insertion loss, high quality-factors, and easy integration in planar radio frequency components. Therefore, it can further reduce the circuit, allowing SIW FAs to be applied in many aspects such as the 5G (5th generation mobile communication technology) and wireless local area network communications.

INDEX TERMS Substrate integrated waveguide (SIW), filtering antenna (FA), multi-mode, incomplete mode, multi-layer, slow-wave technology.

I. INTRODUCTION

Radio frequency (RF) front-end system is an evolving technical solution to support high-performance wireless communication systems. In traditional RF front-end systems, separate components are usually employed, such as filters and antennas. Nevertheless, these separate devices would make the system bulky and costly. Besides, there are also additional losses at the connection of the two devices. The development of modern requires small size, low cost, low loss. Therefore, to meet the above requirements, the filtering antenna (FA) that integrates the filter and antenna is proposed. In addition, to further optimize the transition part between the FA and planar circuit, the substrate integrated waveguide (SIW)

structure is proposed in [1] and [2]. As shown in Fig.1, its specific structure mainly consists of two parallel metal plates, a dielectric substrate, and a series of metallic vias. The influence of bandgap loss can be eliminated by adjusting the distance between metallic vias. On the one hand, the SIW structure retains the advantages of the traditional waveguide, such as the high quality-factor and the high-power capacity, while reducing the circuit size to a large extent. Furthermore, as it is easier to integrate with other devices, there is no need for transitions between components, making the overall system less lossy. Therefore, the SIW technology has advantages in small size, low cost, low loss systems and reduces the total requirement for transition. After a series of improvements, the SIW can be applied to filters [3], [4], antennas [5], [6], power amplifiers [7], [8], power divider [9], oscillators [10] and polarizers [11]. It is apparent that the SIW structure can be

The associate editor coordinating the review of this manuscript and approving it for publication was Mohammad Tariqul Islam .

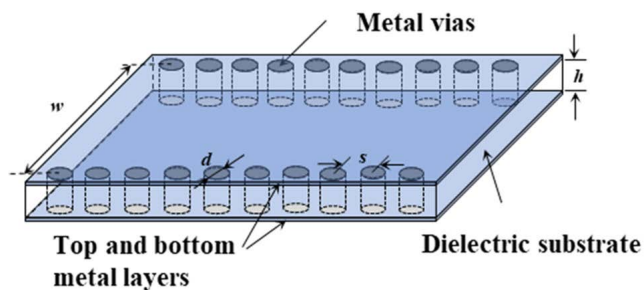


FIGURE 1. Geometry of the classical SIW structure, with the relevant geometrical dimensions.

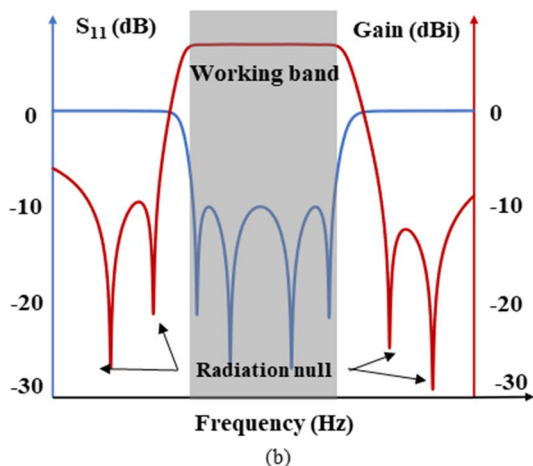
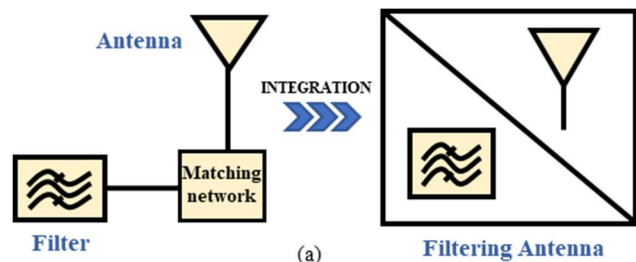


FIGURE 2. (a) Implementation of internal integration of filter and antenna, (b) the curves of return loss and gain.

utilized in the RF front-end as a standard waveguide. Hence, the SIW has excellent development prospects in the design of different devices.

In traditional wireless systems, filters and antennas are usually designed independently and cascaded directly. Matching networks are used between filters and antennas which would lead to an increase in size and insertion loss (IL). Hence, a great configuration is proposed to integrate the filter and antenna, which can realize the functions of filtering and radiation within a compact structure. The integration of the filter and antenna is shown in Fig. 2(a), and the approximate curves of gain and S_{11} of the FA are shown in Fig. 2(b). In order to further intuitively compare the performance and size differences between filter and FA, as shown in Fig. 3(a), the output end of the filter was connected with 50Ω impedance, and as shown in Fig. 3(c), the output of the FA is etched with a long slot to make energy diffused outward. Since the S_{21}

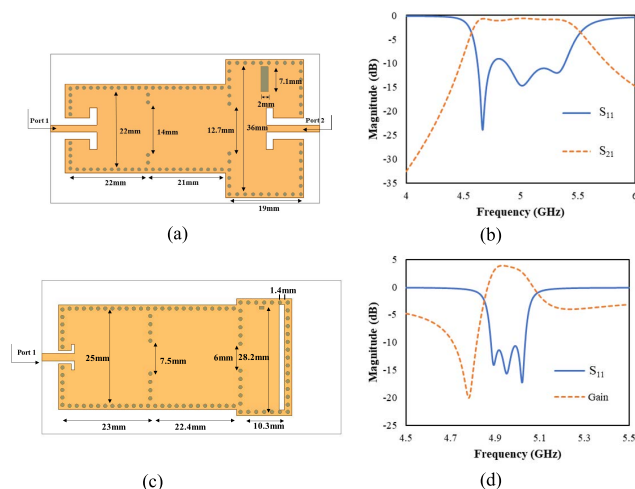


FIGURE 3. (a) Geometry of the filter, (b) simulated S_{11} and S_{21} response of the filter, (c) geometry of the FA, (d) simulated S_{11} and gain of the FA.

parameters of the filter and the gain of the FA have similar port characteristics, a comparison between them can be obtained. As shown in Fig. 3(b) and (d), the S_{21} parameters of the filter are 0dB at the center frequency of 5GHz, while the gain of the FA is 3.27dB under the same configuration. In S_{11} curve, both FA and filter are third-order curves. It can be seen that FA has a gain, and the filter will inevitably lose part of its energy during transmission. By comparing the model diagrams of the two devices simultaneously, it can be seen intuitively that the filter size is slightly larger than that of FA in similar indicators.

Since the massive demand for wireless communication and information service, the explosive growth of corresponding wireless communication systems leads to the increasing demand for compact, low cost, and low power wireless devices. Among them, many compact device designs based on wireless communication system integration modules have appeared. The Web of Science includes more than 10,000 studies on the design of compact devices for wireless communications, so compact is of great importance to integrated circuits. In [12] and [13], the authors designed the embedded filters, the broadband transmitter is designed in [14], and the multi-band antennas are devised in [15] and [16]. They are located in the RF front-end module of wireless communication, which can include integration with other circuit devices expediently. The authors of [17] achieved high performance and compact passive components through the multi-layer ceramic-based thick-film technique. The compact structure of the above devices shows that compactness is an essential characteristic of each independent device in the integration of wireless communication system modules.

In 1929, Plebanski proposed the FA circuit for the first time on the theoretical level [18]. Since then, the research on FAs has been extended to practical circuits. In 1977, Ren *et al.* combined a horn antenna with a filter to form the FA [19]. In 1993, Sanchez-Hernandez *et al.* added the filter to the edge of a patch antenna to achieve dual-frequency [20].

In addition, Abbaspourt-Tamijani *et al.* integrated a patch with a coplanar waveguide transmission line to form a FA. In 2002, a last-stage resonator was replaced with a resonant antenna [21]. In 2003, Queudet *et al.* proposed an idea of leakage waveguides as radiation structures and obtained a preliminary structure of loss-coupling between resonators [22]. The SIW FA are commonly used in the FA, the metal waveguide FA, the microstrip FA. Generally, the order of metal waveguide FA can be increased by repeating elements to form the periodic structure. There are two main methods to integrate the waveguide filter with the antenna structure, one is etching the radiation slot on the top of the waveguide and the other is opening the last stage of the cascade resonator. Comparing with other filters, it has better filtering characteristics, and it is easier to form multi-pass bands. However, as each resonant cavity cascade usually forms a metal waveguide FA, it usually has a lamination for its size and gain in the design [23], [24], [25], [26], [27], [28], [29], [30]. The microstrip FA utilizes the patch antenna as the last stage of the resonator, or etches a specially shaped slot on the top to diffuse the energy outward. Its advantage lies in its small size and simple structure. However, the filtering band of the microstrip FA is limited, the filter order is low, and the S-curve is unsatisfactory in the band. Besides, the design is too complicated, and there are too many parameters in each microstrip line [31], [32], [33], [34], [35], [36].

The authors of [37] and [38] analyzed the normative parameter of the SIW structure in leakage characteristics and wave guidance. As shown in Fig. 1, the bandgap and leakage loss may be generated because the SIW structure is flanked by the metallized via connecting the upper and lower metal plates. In order to reduce these losses, the following design rules need to be considered [37].

$$s > d \tag{1a}$$

$$s/\lambda_c < 0.25 \tag{1b}$$

$$\alpha_1/k_0 < 1 \times 10^{-4} \tag{1c}$$

$$s/\lambda_c > 0.05 \tag{1d}$$

where s is the gap between two adjacent vias, d is the diameter of the via, λ_c is the cut-off wavelength, α_1 is the total loss, and k_0 is the wave number in vacuum. Equation (1a) suggests that the gap between two adjacent (s) must be larger than the diameter (d) so that the circuit is physically realizable. Equation (1b) is required to avoid the bandgap loss in the working bandwidth. The leakage energy can be ignored by the leakage condition Equation (1c). The final Equation (1d) is not necessary but ideal, specifying that it is best to have no more than 20 vias in a wavelength. In Fig. 4, the shaded areas are functions of s/λ_c and d/λ_c in the SIW structure with almost no energy leakage.

SIW has the similar field and dispersion characteristics to traditional waveguides when the metallized vias are closely arranged without energy leakage. However, due to the gap in the SIW side wall, a stable current cannot be formed. It only can transmit the TE mode. The authors of [38] inferred the

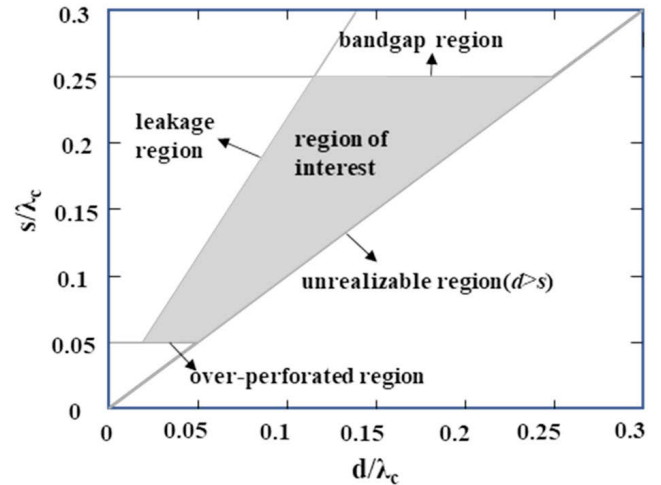


FIGURE 4. Region of interest for the SIW structure as a function of d/λ_c and s/λ_c [38].

empirical relationship between the diameter of the metallized via, SIW's dimensions, and effective waveguide width (w_{eff}) in Equation. (2).

$$w_{eff} = w - \frac{d^2}{0.95s} \tag{2}$$

where (w_{eff}) is the effective width in the waveguide, w is the width of SIW, d is diameter of metallized via, and s is the gap between two adjacent vias. Furthermore, after further considering the influence of d/w , a more accurate Equation. (3) is obtained.

$$w_{eff} = w - 1.08 \frac{d^2}{s} + 0.1 \frac{d^2}{w} \tag{3}$$

When s/d is smaller than 3 and d/w is smaller than 0.2, the empirical equation is very accurate.

For these defects of the metal waveguide FA and the microstrip FA, the SIW FA can effectively solve these problems. Firstly, for studying the miniaturization of the SIW FA, we compare several methods of the miniaturization of the SIW filter. In the process of the SIW filter miniaturization, the SIW is firstly folded to form a multi-layer structure [39], [40], [41]. Then, a particular structure is etched on the top metal layer to form inductive and capacitive loading. The fundamental mode resonant frequency moves to the low-frequency direction, and the physical size of the filter can also be reduced [42], [43], [44], [45], [46], [47], [48], [49]. Next, the slow-wave technology separates the electric and magnetic fields through the perturbation of the internal metallic vias to form the slow-wave effect, which causes miniaturization [50], [51], [52], [53], [54]. Finally, for the incomplete mode, by cutting a complete mode of SIW, the size can be significantly reduced with the field of unchanged fundamental mode [55], [56], [57], [58], [59], [60], [61], [62], [63], [64].

The SIW FA makes the energy diffuse outwards by adding a special structure on the basis of the original SIW filter. In 2007, Luo *et al.* covered the SIW cavity frequency selective surface (FSS) over the aperture of the original horn

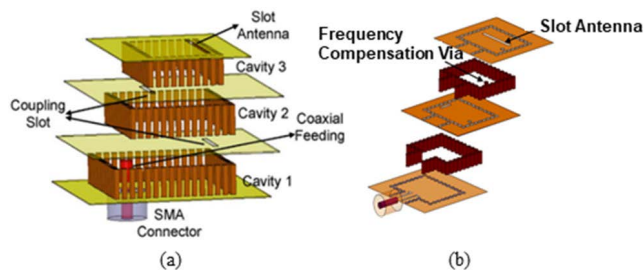


FIGURE 5. (a) Exploded view of a vertically integrated three-pole filter with a slot antenna [70], (b) exploded view of a vertical two-pole cavity filter seamlessly integrated with a slot antenna [71].

antenna, realizing the integration of filtering and radiation, and further reducing the volume and cost of the military platform communication system [65]. To further simplify the design and improve the return loss in the working band, Yu *et al.* proposed a planar FA based on SIW in 2011. The yagi antenna is used in this design, and fifth-order FA is obtained by combining the antenna with the SIW filter [66]. To further reduce the size, Yu *et al.* in 2012 put forward an inductive window bandpass filter and coaxial collinear (COCO) antenna in Ku-band [67]. Also, in 2013, Xue *et al.* proposed a kind of SIW filter and Angle of printed dipole antenna reflector of filtering which can be applied to Q-band indoor short-range wireless communication [68]. Nevertheless, its radiation frequency and gain are still low. In order to overcome the narrow-band characteristics of the SIW FA, Hu *et al.* used two SIW resonant cavities to overlay vertically in 2018. They etched the resonant slot on the top to approach the patch antenna to obtain the third-order FA with high cross-polarization [69].

In the following sections, the miniaturization of the SIW FA is introduced in terms of the mode and physical structure.

II. TECHNICAL REVIEW

A. SIW FA BASED ON MULTI-LAYER

SIW FA based on the multi-layer structure is a common method for miniaturization. Cavities are stacked vertically to reduce the size. The multi-layer structure is easy to meet the physical structure to achieve bypass coupling or source-to-load coupling to increase the radiation null (RN), which will improve the performance of the FA. Compared with other RF devices, since the antenna has only one port, in the manufacture of the multi-layer, there is no need to consider the input and output ports on different layers, which is conducive to integration.

In [70], a third-order FA is firstly realized through three layers. The exploded view of this SIW FA is illustrated in Fig. 5(a). In [71], a novel structure is proposed to realize the highly efficient FA, in which the compensation via in the top cavity is used to adjust the resonant frequency. Using the time-domain technique, the peak value of the time-domain response corresponds to the internal coupling between resonators and the external coupling between resonators and ports. By observing the peak point of the time-domain

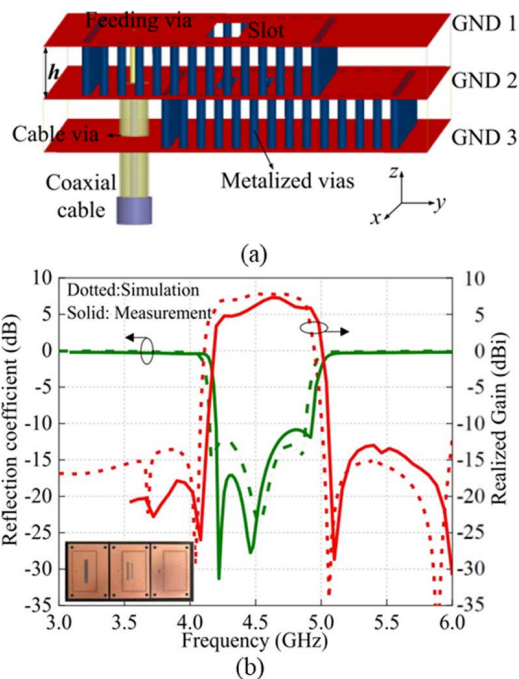


FIGURE 6. (a) Top view of the three metal layers of the proposed antenna, (b) measured and simulated realized gain and return loss of the antenna [72].

response, the parameters in the FA are swept to get the optimal size. As shown in Fig. 5(b), the slot antenna can be formed by etching a slot on the top metal layer. In addition, the authors proposed the equivalent circuit of this FA and gave the calculation relations of coupling coefficient, S_{11} , quality factor (Q), and other factors.

The above studies used simple topologies with no RNs. In order to improve the frequency selectivity, in [72], because of the bypass coupling, a double-coupling scheme was adopted to achieve a FA with four RNs, as shown in Fig. 6(b). As shown in Fig. 6(a), FA miniaturization is realized by double-layer substrate. The dual-slot in the middle metal layer can control the frequency of the RNs respectively. This FA has high frequency selectivity and a wider working bandwidth. However, in the middle of the structure, two RNs must be controlled together by the distance between two slots, and cannot be controlled separately.

The multi-layer technology can make the FA more compact, and hence it can be designed to transmit different information on multiple transmission channels by combining it with the patch antenna. In [73], the authors designed a FA with a four-channel multiplexing operation with two dielectric substrates and a thin foam between them. As shown in Fig. 7(a), a U-shaped slot is etched on the top metal layer, and the four frequencies are divided into high and low frequency bands. The desired four resonant frequencies are generated by adjusting the space between two substrates. Since the SIW cavity is fed directly from the microstrip line, the isolation between ports will deteriorate. Therefore, in order to increase the isolation between several channels, the SIW cavity at the bottom is coupled to the patch through the U-shaped slot to

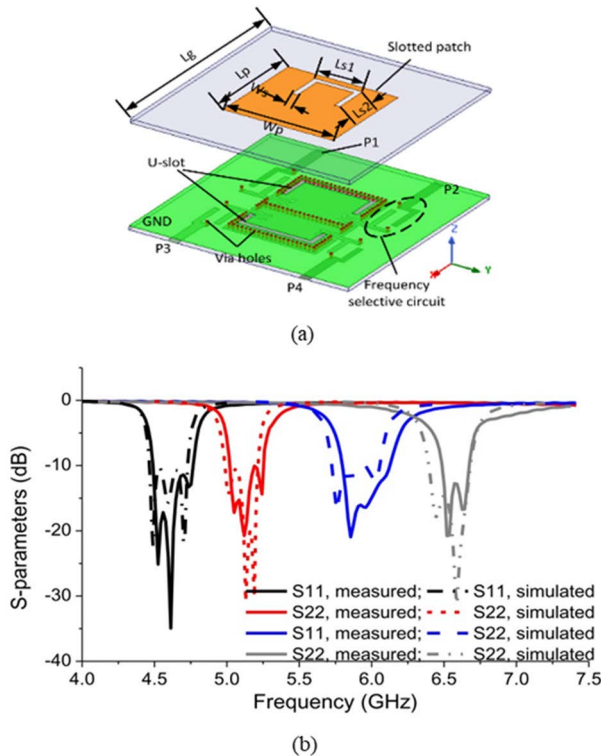


FIGURE 7. (a) Exploded view of the proposed multiplexing antenna, (b) simulated and measured S-parameters of the proposed multiplexing FA [73].

form a filter circuit. However, the radiation efficiency is lower than a conventional antenna. Besides, at high frequencies, as shown in Fig. 7(b), the poles gradually change from three to two.

The multi-channel technology is completed in a cavity as a whole, while the antenna array requires several elements to be reasonably tiled. Through increasing the radiation cavity, we can achieve a high gain of the antenna array. In Fig. 8(a), the authors of [74] etched a slot on the top metal layer of each FA. To keep slot antennas in the same layer to form the array, a multi-layer technique is adopted. The lower SIW cavity is coupled with the upper layer to form a third-order array FA. Nevertheless, the bottom cavity wastes too much space, and the top cavity, which is a cascading form also further increases the overall size. As shown in Fig. 8(b), the authors of [75] constructed a fourth order FA with four layers to further increase the poles of the filter. Furthermore, they etched a horizontal and vertical slot to replace the traditional long slot to realize a dual-polarized antenna.

Furthermore, the authors of [76] combined the multi-layer technology with patch antennas. The FA is formed by two layers of the stacked substrate and a top layer of a right-handed circularly polarized (RHCP) patch antenna. Two cavities are coupled through the coupling slot, and upper cavity is coupled to the patch through the coupling via. Then, the single antenna elements are combined into a 2×2 antenna array, and the patches on the upper layer rotate 90° counterclockwise, respectively. Therefore, this structure can effectively reduce

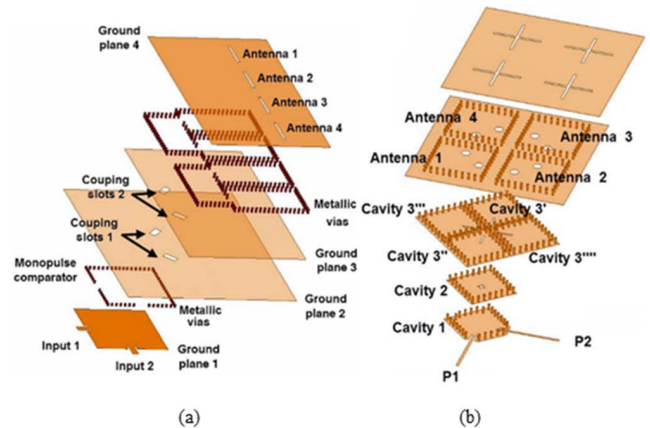


FIGURE 8. (a) Cross-section view of proposed monopoles array FA [74], (b) cross-sectional view of the proposed dual-polarized FA subarray [75].

the thickness of the substrate. However, there is no RN in the structure, so the frequency selectivity is mediocre.

This part mainly introduces SIW FAs by the multi-layer technology. Unlike other microwave devices, the FA formed by the integration of the filter and antenna only has one input port, which is more suitable for using multi-layer technology.

B. MULTI-MODE SIW CAVITY FA

Using multi-mode cavities is an excellent strategy to design SIW FAs with compact size. Because SIW FAs which are based on multi-mode cavities usually have smaller sizes than those based on several single-mode cavities. In addition, since the circular polarization (CP) antenna requires two orthogonal modes, it can be formed by the dual-mode cavity.

The horn FA is formed through the particular outer edge shape of the SIW structure. The authors of [77] used TE_{102} and TE_{201} to achieve two dual-mode cavities in the horn FA. The transmission null (TN) on either side of the working band is realized by the cross-coupling between TE_{101} and TE_{102} modes. However, the TNs cannot be controlled by a single variable. In Fig. 9(a), when $a_1 < w_1$, the filter power divider cavity can be designed as the third resonator, and the last pole is made up of the horn. Adding an improved transition at the end of the structure (the right side of Fig. 9(a)) improve matching, radiation performance and broaden the bandwidth.

In [78], it is also a SIW horn FA, which adopts a conical transition structure. In this horn FA, four rows of inductive metallic vias are embedded into the cavity of the horn antenna thus forming three coupled resonant cavities to achieve the function of the filter. The electric field diagram of each cavity is shown in Fig. 9(b). Besides, the resonant frequency of each cavity is adjusted by changing the distance of metallic via holes. Compared with the traditional H-plane horn antenna, the bandwidth of the proposed antenna is significantly increased. However, the overall dimension is still large, and the design is too complex.

Etching a slot at the maximum electric field of a mode to disturb the resonant frequency in that mode. Therefore, by using this principle, two modes with different resonant

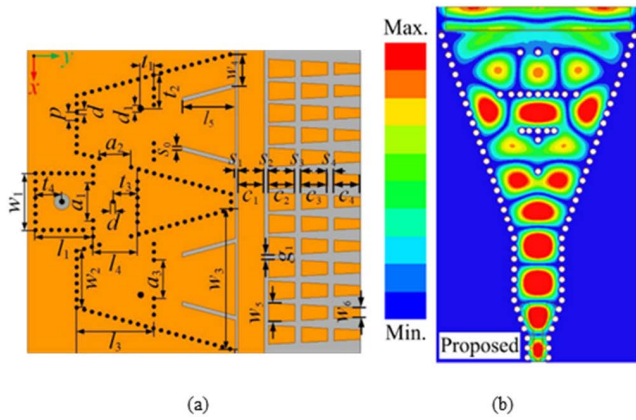


FIGURE 9. (a) Geometry of the proposed FA [77], (b) electric field distributions of the third-order horn FAs with different locations of via holes [78].

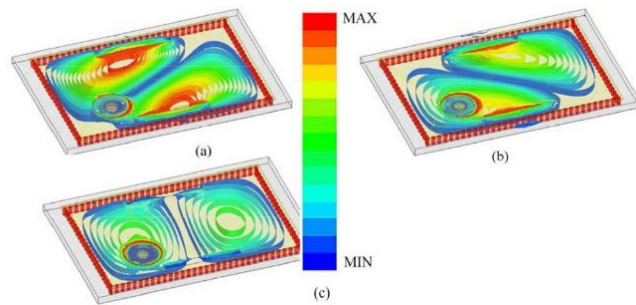


FIGURE 10. Simulated electric field distribution for the dual-mode FA at (a) (b) two poles, and (c) RN [80].

frequencies can coexist in a cavity simultaneously, and the dual-mode cavity technology can be realized. The authors of [79] achieved the CP antenna with TE_{102}/TE_{201} and TE_{103}/TE_{201} dual-mode cavities. Similarly, in [80], a dual-mode FA is implemented on the single-layer SIW and a single cavity without apparent and additional filter structure. In Fig. 10, the two poles are a pair of split modes generated by degeneracy modes of TE_{102} .

In another approach, the multi-layer and multi-mode technology are well combined to reduce the size of the FA. In [81], the authors designed a three-order FA which is composed of two cavities. As shown in Fig. 11, two slots were etched on Ground 2 to form two modes. The electric field of the quasi-cavity mode distributes in the whole SIC and the electric field of the quasi-dual-slot mode is more concentrated near the dual slots. These two modes can change the frequency of the two RNs by controlling the distance between the two slots, forming the upper and lower nulls. Meanwhile, the double slots on the top metal layer radiate energy outwards, while the TE_{110} mode inside the cavity alone cannot radiate energy. Therefore, the flexibility of this design can be improved. Although the resonant frequency of the two modes can be changed by controlling the double slot, it still needs to cooperate with multiple variables, and there is no independent control.

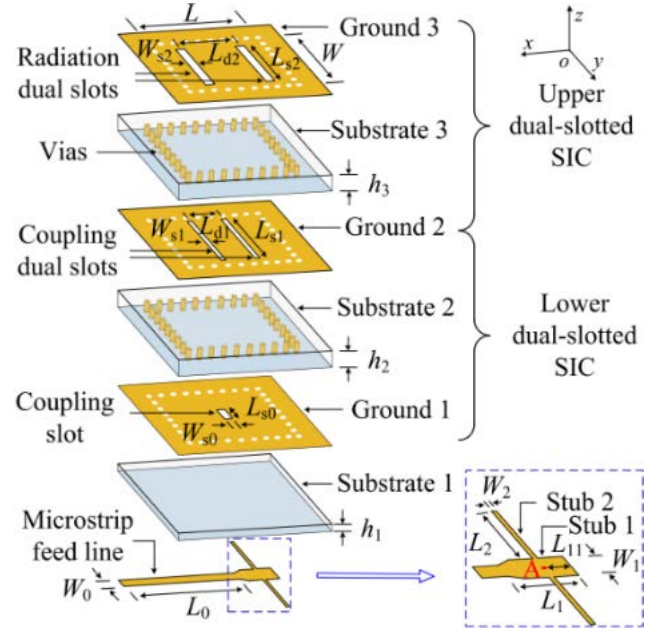


FIGURE 11. Configuration of the proposed antenna [81].

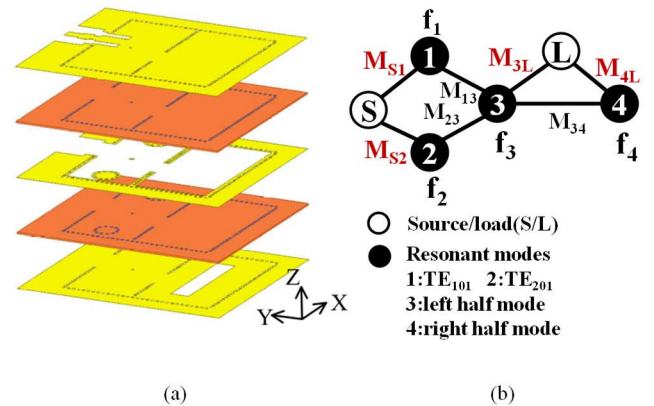


FIGURE 12. The structure of the proposed SIW FA. (a) 3D view. (b) Coupling diagram [82].

Additionally, to etch the slot, some special structures can be added to the maximum electric field, reducing or increasing the resonant frequency to design the dual-mode cavity. In [82], the authors designed a dual-mode SIW cavity based on TE_{101} and TE_{201} modes. The designs achieved controllable RN located on the upper working band, and its topology is shown in Fig. 12(b). Besides, the geometry of the FA is shown in Fig. 12(a). The mushroom structures are etched on the middle metal layer where the maximum electric field of TE_{201} . Therefore, the resonant frequency of TE_{201} mode can decrease faster than TE_{101} mode, and two different modes can coexist in the same cavity. Miniaturization in the conventional SIW cavity resonator can be achieved through these structures. The FA based on a dual-mode cavity and two half-mode cavities is achieved by a slot on the bottom layer. The lower out-of-band RN can be controlled by the distance of the slot from the center.

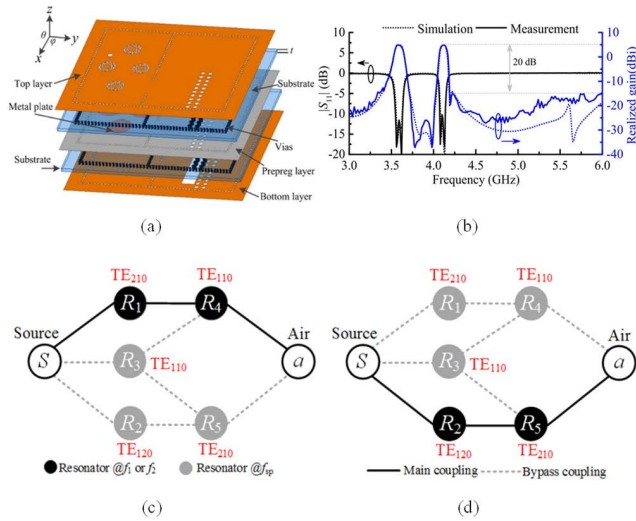


FIGURE 13. (a) 3D view of proposed dual-band SIW FA, (b) simulated and measured reflection coefficients and realized gains of the proposed FA, (c) coupling schemes of the proposed FA at low band f_1 , and (d) high band f_2 [83].

The authors of [83] designed a dual-band SIW cavity with TE₂₁₀/TE₁₁₀ and TE₁₂₀/TE₂₁₀ dual-mode, whose topologies of dual-band are shown in Fig. 13(c) and (d). Two rows of metallic vias arrays are located at the maximum electric field of TE₁₁₀ mode. Hence, the interference to TE₁₁₀ mode is more significant, resulting in the appearance of a dual-mode cavity. The slot next to the array cuts off the current of TE₁₁₀ and TE₂₁₀ modes, creating a potential difference on both sides, which can be used as an external radiation antenna. Fig. 13(a) shows that two dual-mode cavities have similar dimensions. Four special structures named metal-insulator-metal (MIM) capacitors are located at the maximum of each electric field. They can be used to disturb the frequencies of higher-order modes. The dual-mode of TE₂₁₀/TE₁₀₂ has a similar size to the other. The MIM structure reduces the size by 48%. This structure can produce three RNs. The second and third RNs can be moved by adjusting the feeding position. Therefore, it can improve the out-of-band suppression. The size of the proposed FA is further reduced (60.39% miniaturization) by these structures. And the two working bands as shown in Fig. 13(b).

A center-fed SIW cavity-backed slot antenna can support a resonant with conical radiation patterns, but its bandwidth is too narrow. In order to increase the bandwidth, the authors of [84] investigated SIW cavity-backed slot and patch antennas, as shown in Fig. 14. And compared with patch antennas, the cavity-backed patch antenna has higher gain. The mode of this design includes the patch TM₀₁ mode, the cavity TM₀₁ mode, and the cavity TM₀₂ mode. Through combining these three modes, a triple-resonance FA with wide bandwidth can be obtained. When the substrate thickness is large enough, the mode of the cavity can be excited effectively to form a wide bandwidth. However, the frequency selectivity of this structure becomes worse, and two kinds of TM₀₁ modes are hard to be distinguished in the curve of return loss.

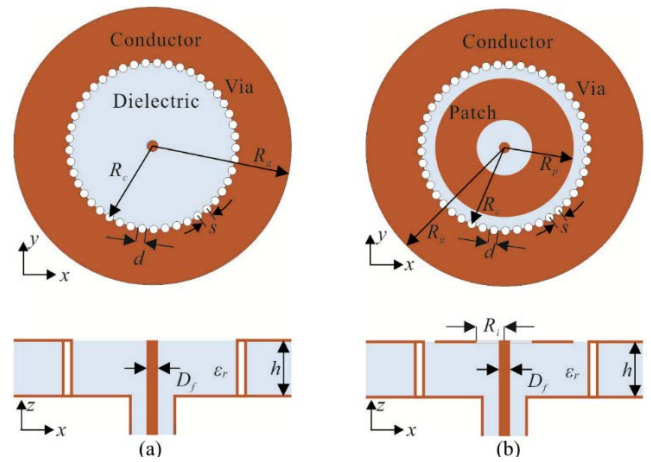


FIGURE 14. Geometries of (a) the SIW cavity-backed slot antenna, and (b) the SIW cavity-backed gap-coupled patch antenna [84].

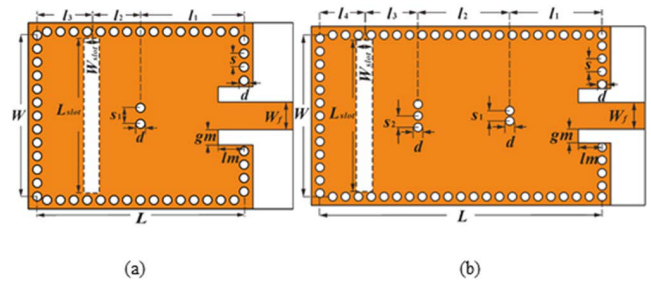


FIGURE 15. Configuration of the proposed (a) triple-resonance antenna, (b) quad-resonance antenna [86].

Through changing the space of traditional SIW vias and enlarging the size of the top metal layer by folded configuration, the authors of [85] constructed a 1/4 wavelength patch on the top metal layer with a SIW dual-mode (TE₁₀₂/TE₂₀₁) cavity to achieve a third-order FA. By using the folded configuration, the antenna does not occupy additional ground dimensions. The size of the proposed FA is 69.08% smaller than other common FA. There are two parasitic modes out of the working band, one is a lower TE₁₀₁ mode which is suppressed by the shorting vias, and the other is the higher order mode at a higher frequency of the working band. When the space of sparse vias becomes larger, the Q of the SIW cavity decreases. By adjusting the position of the center asymmetrical shorting pins, the shorting pins were equivalent to a load inductance, which can improve impedance matching and axial ratio (AR) bandwidth.

The author of [86] divided the complete mode into multi-mode cavities by loading shorted-end vias into a single cavity. By etching slots on the metal layer, the third-order FA consists of half-TE₁₁₀, odd TE₂₁₀ and even TE₂₁₀ mode. The half-TE₁₁₀, odd TE₂₁₀, even TE₂₁₀ and TE₃₁₀ mode compose the fourth-order FA. The structures of the two designs are shown in Fig. 15(a) and (b). However, this FA has no RN. Hence, although the bandwidth is high, the frequency selectivity becomes worse.

In summary, in most cases, multi-mode technology combined with multi-layer technology can effectively optimize

the performance of the SIW FA on the original basis. As shown in [87], combining the two technologies allows a new topological structure to obtain more required nulls and increases the out-of-band suppression. A similar approach can also be applied to SIW FAs. The single-layer structure combined with multi-mode technology can produce multiple poles in a cavity, making the TN narrow. In the construction of a dual-mode cavity, in many cases, a special structure is loaded at the maximum electric field of one mode so that the structure can disturb the electric field, and the dual-mode cavity can be constructed to a large extent. This method has been applied in [88], and the result becomes ideal, even without changing the original physical size.

C. SIW CAVITY FA WITH INCOMPLETE MODE CAVITY

In general, an incomplete cavity can significantly reduce the circuit size. The circuit size only accounts for half of the complete mode by using the half mode technology. Furthermore, the quarter mode can save three-quarters of the space. The complete mode cavity can be divided into several incomplete cavities by etching slots on the metal layer at the top or bottom. The FA can also be miniaturized by using the incomplete mode. Furthermore, in many cases, etching slots introduce RNs thus further improving frequency selectivity. In addition, when the position of the etching slot of the partially constructed incomplete mode changes within a specific range, the original generated RN can be controllable, increasing the flexibility of the design requirements for the result.

In those mentioned above, the authors of [79] improved the original TE₁₀₂/TE₂₀₁ dual-mode cavity of the SIW FA into a half-mode SIW (HMSIW) with an incomplete mode, further reducing the circuit size. The original rectangular slot is improved into an elliptical slot to allow the current to flow more smoothly along the edges, thus improving efficiency. This structure can reduce the SIW dimensions by 62.64% of the conventional SIW structures.

In [89], a third-order filter is designed by four metalized posts in the middle to divide the TE₁₂₀ mode resonators into two TE₁₁₀ modes. Besides, as shown in Fig. 16(a), the slot is etched on one side to split one of the TE₁₁₀ modes into two half TE₁₁₀ mode resonators. By adjusting y_s , as shown in Fig. 16(b), the skirt selectivity can be enhanced by moving the RN close to the working band. Moreover, RN can be moved from one side of the working band to the other by changing the slot position.

The incomplete mode SIW cavity and multi-layer SIW can combine in [90]. The topology of the structure is shown in Fig. 17(c). The coupling matrix represents the filtering network, and the coupling matrix is normalized by the coupling coefficient, external Q (Q_e), and other characteristic values. The relationship between the coupling coefficients and the structural parameters of the resonators is studied. According to the theoretical and numerical analysis, the expected double-passband filter response can be obtained using an appropriate physical structure. When port 1 is excited, the

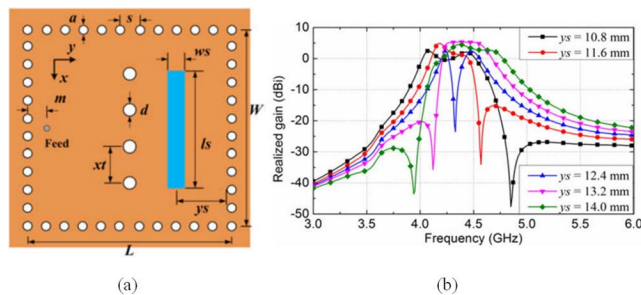


FIGURE 16. (a) Top view of configuration of the proposed antenna, (b) effect of the slot offset y_s on realized gain [89].

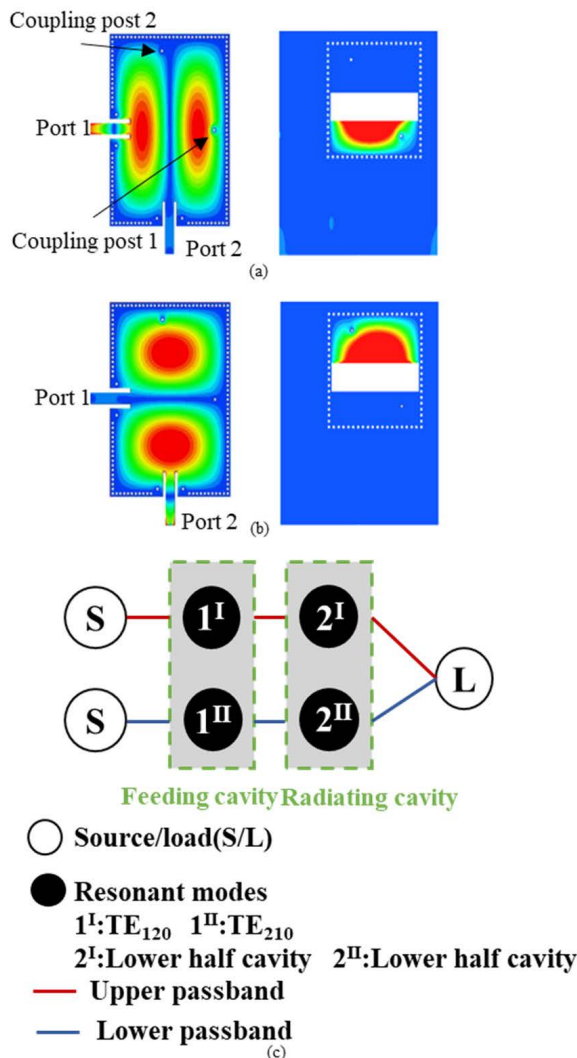


FIGURE 17. Simulated E-field magnitude distributions in feeding and radiating cavities when (a) Port 1 is excited, (b) Port 2 is excited, (c) coupling topology of the proposed duplex FA [90].

feed cavity TE₁₂₀ and the coupling post 1 are used to couple the lower half cavity of the upper substrate to form an upper working band second-order filter. When port 2 is excited, coupling post 2 and the feed cavity TE₂₁₀ coupling the upper half cavity of the top substrate form a lower working band. The electric field are shown in Fig. 17(a) and (b). Two orthogonal

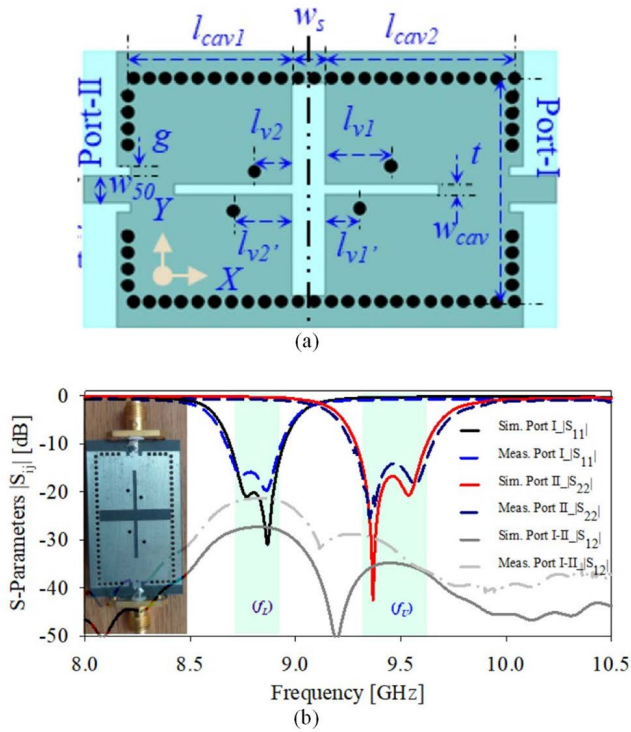


FIGURE 18. (a) Top view of proposed duplex-FA, (b) simulated and measured $|S_{ij}|$ parameters and fabricated sample [91].

modes were used to realize the common feeding cavity in the design. The common radiating cavity is converted into two half-mode cavities by etching rectangular slots. At the same frequency, only half of the radiating cavities in the upper cavity are effective radiators. To some extent, this also led to the waste of space.

Based on the above FA, to further reduce the size, the authors of [91] proposed a second-order duplex FA with a single layer made by using an incomplete mode. A wider vertical slot and a thinner horizontal slot are etched in the center of the top metal layer. The wide slot divides the single band into high and low frequency bands, as shown in Fig. 18(a), and the thin slot improves HMSIW into a dual-mode cavity. Moreover, controlling the position of the loaded-vias loaded near each slot can enhance the selectivity of the working band and strengthen the port isolation. However, the poles in each band cannot be controlled individually, and the resulting two bands can vary only in small ranges. The S-Parameter of the FA is shown in Fig. 18(b). This structure can greatly reduce the circuit size by 62.08%.

In addition to split a cavity into two parts, it can be divided into several parts. This enables the filter to generate more poles, thus achieving optimal performance. The authors of [92] split the single-cavity into three parts, as shown in Fig. 19(a). At different frequencies, the electric field is concentrated in different sub-cavities, and the magnitude in other sub-cavities is negligible. These two slots combined with the capacitively coupled feeding disc excite four modes, three of which increase the impedance bandwidth. The fundamental

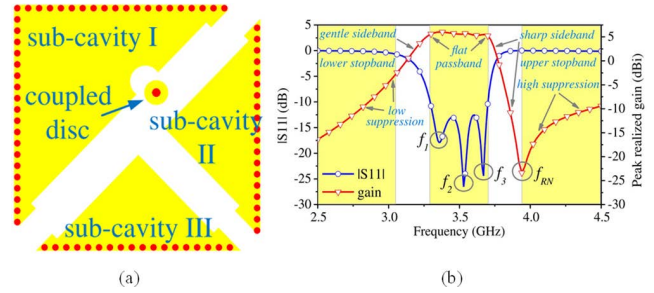


FIGURE 19. (a) Exploded mode of proposed antenna, (b) simulated $|S_{11}|$ and peak realized gain of the proposed design [92].

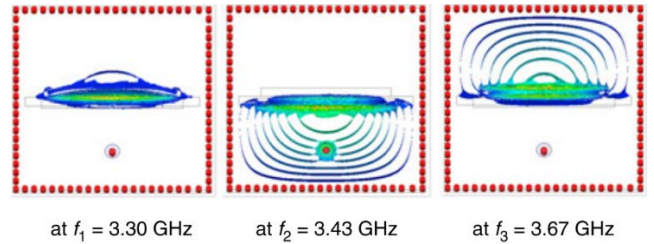


FIGURE 20. Electric field scalar distributions at three resonant modes [93].

mode is the no radiating mode to achieve a RN and produce high stopband suppression. Therefore, the energy of three frequencies in the cavity is excited, thus forming a third-order filter. The RN can be easily adjusted by controlling the feeding position, thus producing a high radiation suppression in the stopband. However, this controllable RN only appears above the working band, and there is a certain limit to the frequency selectivity.

Alternatively, two long parallel slots can be etched on the metal layer. In [93], two slots are etched on the top and a longer slot on the bottom metal layer, the resonant frequencies of the two original modes are significantly reduced. The electric fields at the frequencies of the three poles are shown in Fig. 20. This structure produces an upper RN and a lower RN controlled by the position of the long slot, which results in a quasi-elliptic filtering response. In addition, to obtain good radiation patterns, there are slight overlaps between the two top slots and the bottom slot. However, both RNs are controlled by the same variable and cannot be changed independently.

In [94], etching a long slot on the middle metal layer will divide a cavity into two half-modes and make the middle cavity achieve a dual-mode resonator, as shown in Fig. 21. A short slot on the side produces two controllable TNs, and the l_7 and W_4 control lower and upper RNs, respectively. A patch antenna is added to the top layer to form TM_{010} as the third resonant mode. And shorting pins is added to the upper cavity to improve the gain and reduce the H-plane cross-pol. The device size is reduced by about 65.53% compared to conventional devices through the dual half-mode cavity.

The authors of [95] firstly designed a cascade of second-order filter and etched a slot on the center of the metal layer in the second cavity. When the third-order FA is formed, the

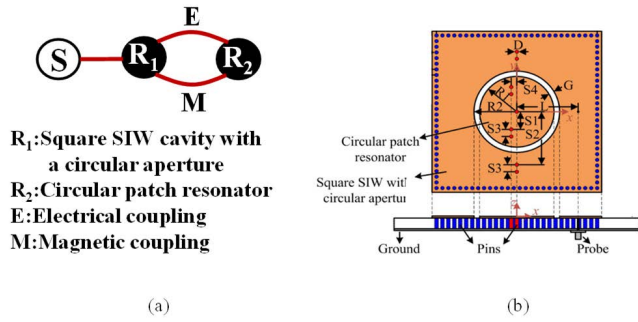


FIGURE 24. (a) Schematic topology of antenna, (b) configuration of the proposed antenna [97].

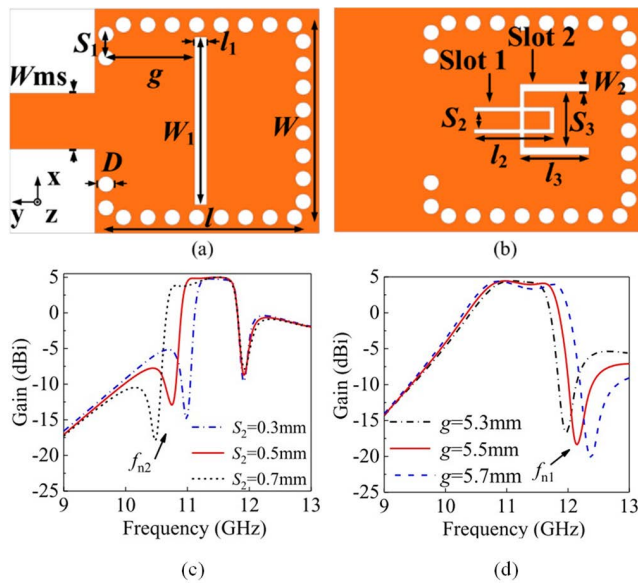


FIGURE 25. Geometry of the proposed FA (a) top surface, (b) bottom surface, (c) frequency RN f_{n2} varies with S_2 , (d) frequency of RN f_{n1} varies with g [98].

implemented a third-order FA with two U-shaped slots and one long slot. As shown in Fig. 25(a) and (b), the long slot caused a single cavity to produce a dual-mode cavity with an out-of-band RN. U-shaped slot 1 caused the FA to generate a below RN to increase frequency selectivity. U-shaped slot 2 made the right half cavity excite the half- TE_{110} mode. The electric field of this mode is compressed in the cavity to generate resonant frequency points at higher frequencies, thus causing three poles to increase the bandwidth. The upper and lower RNs are controlled by g and S_2 , respectively. However, as shown in Fig. 25(c), these two RNs are not controllable. These nulls change as the overall bandwidth changes. Overall, U-slot can reduce the FA by 81.4% compared with the control group in this paper.

In addition to combining two U-slots, one U-slot can also be modified to produce a special structure. In [99], The U-slot makes the SIW cavity form the electric and magnetic mixed coupling. Loading electric and magnetic mixed coupling structures weakens the strength of TE_{120} , which leads to unequal magnitude of TE_{120} on the two sides of the slot. The fundamental and TE_{120} modes interact, and their magnetic

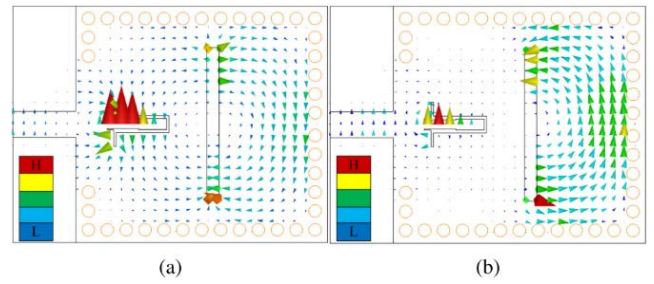


FIGURE 26. The distribution of H-field (a) TE_{120} mode, (b) electric and magnetic mixed mode [99].

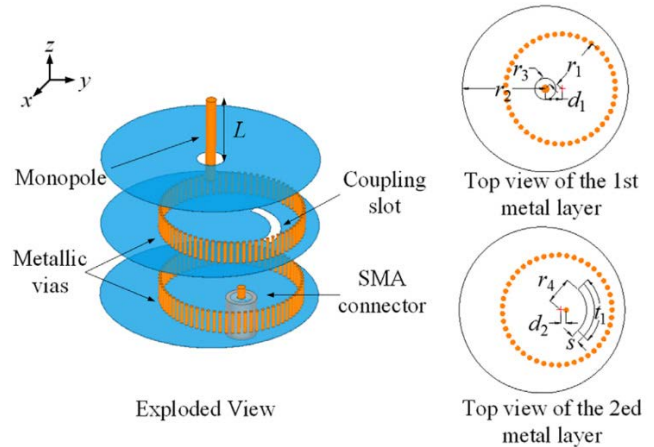


FIGURE 27. Expanded view of the proposed FA, and top view of the first and the second metal layer [100].

fields cancel each other. The magnetic field in the left slot weakens, producing an electric and magnetic mixed mode, as shown in Fig. 26. The coupling structure is not in contact with the cavity and can form electrically coupling. The electric and magnetic mixed coupling structure is shared with the cavity and can form magnetic coupling, generating the upper RN. The current on the both sides of the slot is equal magnitude and in opposite. Therefore, there is no transverse radiation. The extended length below the U-shaped slot controls the lower RN. However, the lower RN change is based on the bandwidth and not controllable in the practical sense.

In addition to the overall rectangular SIW cavity, it can also be directly designed to be circular. The authors of [100] composed a FA of a monopole and two stacked annular waveguide cavities can reduce the dimensions by 32.38%, as shown in Fig. 27, to achieve a third-order FA. The upper RN results from cross-coupling the source and the non-adjacent resonator. By changing r_4 and t_1 , the frequency of the RN can be controlled.

In summary, some SIW FAs with the hybrid structure are introduced. On the one hand, the order of the FA is increased, or the bandwidth is flexible by adding a particular structure. On the other hand, by changing the external shape of the whole structure, a new resonance mode is introduced to construct a SIW FA which is different from the traditional rectangular shape.

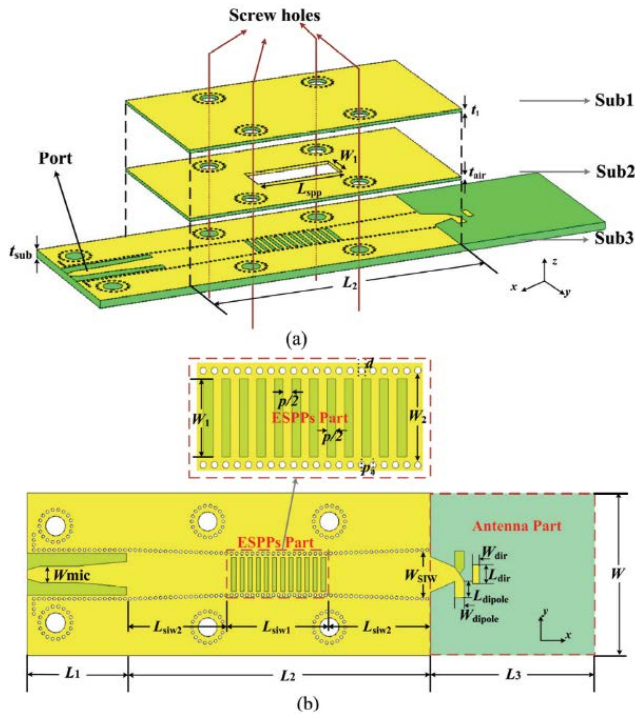


FIGURE 28. Geometry of the proposed ESPPs-SIW FA (a) 3-D view, (b) top view of SIW [111].

E. SLOW-WAVE FA

In addition to the slow-wave technology of loading internal metallic vias mentioned above, surface plasmon polaritons (SPPs) structure can also be loaded to achieve the slow-wave technology [101], [102], [103], [104], [105], [106], [107]. In [108], the authors proposed a new type of SIW-SPP composite guided wave transmission line and used this transmission line to construct a bandpass filter. Combining the SIW with effective surface plasmon polaritons (ESPPs) improves bandwidth flexibility and provides a stable stopband. ESPPs can propagate along the interface of the effective epsilon-negative and the epsilon-positive structures. This structure has a certain foundation in the SIW filter. In [109], the authors tried to propagate in SIW of different dielectrics. In [110], a dual-band filter based on two different ESPPs modes was constructed, but the bandwidth was not controlled by independent parameters.

As shown in Fig. 28, in [111], the structural length L_{SPP} of ESPPs mainly affects the out-of-band suppression of the filter, and the bandgap between the ESPPs causes the stopband performance of the filter. The width of SIW and the filling dielectric can control the start frequency of the working band. These can achieve the purpose of controllable bandwidth. Therefore, the authors design a filter based on ESPPs induced by structural dispersion and combine it with a yagi antenna to construct a FA with controllable bandwidth and a stable stopband. Therefore, the design of this structure can be used to fabricate UWB FAs.

To sum up, comparison of the different miniaturization techniques in SIW FAs is presented in Table. 1.

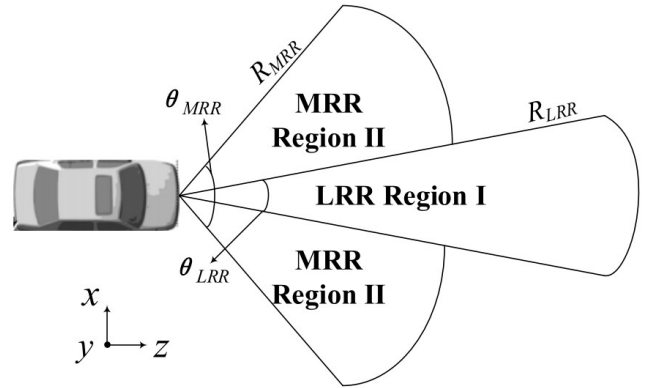


FIGURE 29. Operational zone of MRR and LRR [113].

III. APPLICATION

With the technology matures, SIW FAs have been gradually transferred from academia and research institutions to industrial R&D departments and commercial suppliers. From the beginning of the SIW technology development to the present, SIW FA is mainly used in 5G (5th generation mobile communication technology) and wireless local area network (WLAN) communication, as well as the satellite radar. Because of the advantages of high gain and wide bandwidth, the array antenna is an ideal choice for the above practical applications.

In the early stage, a X-band SIW array FA for radar was firstly studied in [112], and then the application of SIW FA array in automotive radar was studied. As shown in Fig. 29, there is the application scope of the vehicle medium-range radar (MRR) and long-range radar (LRR). The array in [113] used a 1×16 SIW slot as a unit. Due to the bandwidth requirements of LRR, the array is composed of six identical SIW arrays, and the antenna can support MRR and LRR at the same time. The electromagnetic energy is fed to the 2×4 array using the metallic blind holes and metallic vias from the power divider in [114]. Meanwhile, changing the shape and position of the metal layer slot at the top and combining the eight-channel SIW. Then, the wideband millimeter-wave SIW cavity-backed slot array antenna can be obtained which is suitable for 79 GHz automotive radar.

Due to its relatively small size, SIW array FAs has been widely used in ground communications such as 5G and WLAN. As 5G is applied in the 28 GHz band, the path loss is severe. Hence, directional antennas or phased arrays need to be designed for achieving the desired SNR. Generally, the array configuration for 5G applications mainly includes a linear array and a rectangular array. However, this array has a fixed asymmetry and the main lobe of the rectangular array radiogram has again fluctuation of about 35 dB under different azimuth cutting. Therefore, the authors of [115] used the circular structure, and the circular array has a symmetric structure, to achieve stable and high gain. In wireless communication systems, radial line slot array (RLSA) antenna has become a popular antenna suitable for wireless communication systems because of its flat and low-profile

TABLE 1. Comparison of different miniaturization techniques in SIW FAs (FBW = fractional bandwidth, and NA = not available).

Ref	Miniaturization Technique	Size Reduction (%)	Order	Center Frequency (GHz)	FBW (%)	Selectivity	Gain
[70]	Multi-layer	N.A.	3	10.07	5.5	Low	6.0 dBi
[72]	Multi-layer+HMSIW	N.A.	3	4.5	15.4	High	7.5 dBi
[75]	Dual-patch+dual-polarized	N.A.	4	37.07	1.43	Low	10.8 dBi
[77]	Dual-mode	40.68	4	16.1	12.2	High	12.8 dBi
[79]	Dual-mode (TE ₁₀₂ /TE ₂₀₁)	41.21	2	10	3.3	Low	7.0 dBic
	HMSIW(elliptical slot)	62.64	2	10	4.1	Low	7.5 dBic
	Dual-mode (TE ₁₀₃ /TE ₂₀₁)	5.09	2	10.2	2.0	Low	7.1 dBic
[81]	Dual-slot	7.84	3	9.67	9.1	High	7.2 dBi
[83]	Dual-mode(MIM+via-holes array)	60.39	2	3.59/4.11	2.3/1.6	High	4.84dBi/4.85dBi
[85]	Folded CP antenna	69.08	3	5.03	7.2	Low	8.0 dBic
[90]	HMSIW+Dual-mode	16.28	2	4.1/4.9	3.2/3.9	Middle	4.36dBi/4.83dBi
[91]	HMSIW	62.08	2	8.33/9.52	3.0/4.2	Middle	4.48dBi/4.66dBi
[92]	Unequal sub-cavity	8.48	3	3.52	12.5	Middle	5.24 dBi
[93]	Dual-HMSIW	65.53	3	3.61	12.6	High	9.06 dBi
[98]	U-slot	81.4	3	11.8	11.84	middle	5 dBi
[100]	SIW+monopole	32.38	3	5.48	16.4	middle	1.1 dBi
[111]	ESPPs-SIW	N.A.	5	24.91	29.3	middle	8 dBi

characteristics. In [116], the disk structure is also employed to design an RLSA antenna for wireless communication through the SIW structure.

Furthermore, for the multiple input multiple output (MIMO) system, a rectangular SIW array antenna is proposed to avoid mutual coupling between antennas [117]. Similarly, using the advantages of the SIW antenna, [118] designed a slotted SIW array antenna which is suitable for WLAN. The antenna surface adopts several longitudinal slot array structures. By optimizing the number of branches in an array and the number of slots in one SIW branch, the gain can meet the desired requirements.

IV. CONCLUSION

In this paper, the latest development and miniaturization techniques of SIW FA are reviewed in detail. The advantages of integrated FA compared with discrete filter and antenna are introduced. By combining with many different SIW FA examples, different methods of reducing circuit size

are explained. The results show that the miniaturization technology can be realized by using the multi-layer, multi-mode, incomplete mode and slow-wave technology, as well as the summarized hybrid technology (sub-mode and other miniaturization techniques).

So far, array antennas have been used to miniaturize SIW FA in practical applications, while other SIW FA miniaturization methods are still in the theoretical research stage. In order to achieve the miniaturization of the SIW FA, dielectric substrates with high permittivity can be selected. In addition, the FA can be further miniaturized by creating more new topologies and combining known topologies into multi-mode structures. Similar to [55], the multi-mode technology and slow-wave technology have been relatively mature in SIW filters, and the SIW FA can also refer to the miniaturization methods which are commonly used in filters. Nevertheless, miniaturization inevitably reduces the Q and IL. In most cases, materials, structures, and patterns should be balanced so that the final structure can be as small as possible.

Processing costs and other factors have no significant effect on the advantages of the SIW structure.

The FA and its miniaturization technology can meet the requirements of current and future wireless communication systems. Compared with the traditional combination of filter and antenna, the FA in the communication system is more efficient in terms of the size, cost, and loss of the whole subsystem. We believe that tunability and reconfigurability will play an essential role in achieving the flexibility of SIW FA structures. They are typical of particular interest to the multi-band and multi-mode FA. The SIW can easily accommodate tuning devices or materials through field-circuit interactions in the individual electric and magnetic tuning/switching. Combining the multi-layer technology provides more space for tuning devices or materials to accommodate and drive. Therefore, the constructed FA tends to be idealized in a certain range by controlling the tuning devices or materials.

In addition, it can be known from [119] and [120] that the conductor and medium losses can be enhanced by using the complementary split-ring resonator (CSRR), and the energy can be fully absorbed by using the inherent loss of materials, so as to realize the common-mode absorption of broadband. In this way, the reflection of energy is suppressed. Therefore, CSRR combined with SIW structure and artificial microstructure design is expected to realize the absorption filter. According to the method mentioned above, the SIW FA can be further designed to meet the design conditions.

REFERENCES

- [1] D. Deslandes and K. Wu, "Integrated microstrip and rectangular waveguide in planar form," *IEEE Microw. Wireless Compon. Lett.*, vol. 11, no. 2, pp. 68–70, Feb. 2001, doi: [10.1109/7260.914305](https://doi.org/10.1109/7260.914305).
- [2] D. Deslandes and K. Wu, "Single-substrate integration technique of planar circuits and waveguide filters," *IEEE Trans. Microw. Theory Techn.*, vol. 51, no. 2, pp. 593–596, Feb. 2003, doi: [10.1109/TMTT.2002.807820](https://doi.org/10.1109/TMTT.2002.807820).
- [3] H.-Y. Chien, T.-M. Shen, T.-Y. Huang, W.-H. Wang, and R.-B. Wu, "Miniaturized bandpass filters with double-folded substrate integrated waveguide resonators in LTCC," *IEEE Trans. Microw. Theory Techn.*, vol. 57, no. 7, pp. 1774–1782, Jul. 2009, doi: [10.1109/TMTT.2009.2022591](https://doi.org/10.1109/TMTT.2009.2022591).
- [4] A. Iqbal, A. W. Ahmad, A. Smida, and N. K. Mallat, "Tunable SIW bandpass filters with improved upper stopband performance," *IEEE Trans. Circuits Syst. II, Exp. Briefs*, vol. 67, no. 7, pp. 1194–1198, Jul. 2020, doi: [10.1109/TCSII.2019.2936495](https://doi.org/10.1109/TCSII.2019.2936495).
- [5] G.-G. Namgung, C. Lee, H. Park, Y. Seo, S. Kahng, and D. Lim, "Design of wideband SIW beamforming circularly polarized antennas for 5G-band," in *Proc. 8th Asia-Pacific Conf. Antennas Propag. (APCAP)*, Aug. 2019, pp. 297–298.
- [6] L.-R. Tan, R.-X. Wu, and Y. Poo, "Magnetically reconfigurable SIW antenna with tunable frequencies and polarizations," *IEEE Trans. Antennas Propag.*, vol. 63, no. 6, pp. 2772–2776, Jun. 2015, doi: [10.1109/TAP.2015.2414446](https://doi.org/10.1109/TAP.2015.2414446).
- [7] Z. Wang and C.-W. Park, "Novel substrate integrated waveguide (SIW)-based power amplifier using SIW-based filter to suppress up to the fourth harmonic," in *Proc. Asia Pacific Microw. Conf.*, Dec. 2012, pp. 830–832.
- [8] Z. Wang and C.-W. Park, "Novel substrate integrated waveguide (SIW) type high power amplifier using microstrip-to-SIW transition," in *Proc. Asia-Pacific Microw. Conf. Proc. (APMC)*, Nov. 2013, pp. 101–103.
- [9] H. Chen, W. Che, X. Wang, and W. Feng, "Size-reduced planar and nonplanar SIW Gysel power divider based on low temperature co-fired ceramic technology," *IEEE Microw. Wireless Compon. Lett.*, vol. 27, no. 12, pp. 1065–1067, Dec. 2017, doi: [10.1109/LMWC.2017.2765558](https://doi.org/10.1109/LMWC.2017.2765558).
- [10] Z. Cai, X. Tang, T. Zhang, and Y. Yang, "An X-band low phase noise oscillator with high harmonic suppression using SIW quarter-wavelength resonator," in *IEEE MTT-S Int. Microw. Symp. Dig.*, Jun. 2018, pp. 427–430.
- [11] E. Armeri, G. Amendola, L. Boccia, and F. Voci, "TX-RX K/Ka band polarizer based on a SIW polarization twister," in *Proc. IEEE Int. Symp. Antennas Propag. USNC/URSI Nat. Radio Sci. Meeting*, Jul. 2018, pp. 2055–2056.
- [12] Y. Zhou, A. Sun, J. Zhou, and Y. Shen, "A compact multi-channel receiver front-end using SiP integration technology on LTCC substrate for wireless communications," in *Proc. Int. Conf. Wireless Commun. Signal Process. (WCSP)*, Oct. 2015, pp. 1–5.
- [13] T. Matsumura, K. Ibuka, K. Ishizu, H. Murakami, F. Kojima, and H. Harada, "Prototype of IEEE 802.11af-based baseband IC enabling compact device for wireless local area network systems in TV white-spaces," *IEEE Trans. Cognit. Commun. Netw.*, vol. 3, no. 3, pp. 450–463, Sep. 2017, doi: [10.1109/TCCN.2017.2750684](https://doi.org/10.1109/TCCN.2017.2750684).
- [14] M. Ali, A. Jankowski, R. C. Guzman, L. E. G. Munoz, F. van Dijk, and G. Carpintero, "Photonics-based compact broadband transmitter module for E-band wireless communications," in *Proc. 49th Eur. Microw. Conf. (EuMC)*, Oct. 2019, pp. 808–811.
- [15] T. Upadhyaya, A. Desai, R. Patel, U. Patel, K. P. Kaur, and K. Pandya, "Compact transparent conductive oxide based dual band antenna for wireless applications," in *Proc. Prog. Electromagn. Res. Symp. Fall (PIERS-FALL)*, Nov. 2017, pp. 41–45.
- [16] S. Mudda, K. M. Gayathri, and M. Mudda, "Compact high gain microstrip patch multi-band antenna for future generation portable devices communication," in *Proc. Int. Conf. Emerg. Smart Comput. Informat. (ESCI)*, Mar. 2021, pp. 471–476.
- [17] K. K. Samanta, "3D/multilayer heterogeneous integration and packaging for next generation applications in millimeter-wave and beyond," in *IEEE MTT-S Int. Microw. Symp. Dig.*, Dec. 2017, pp. 294–297.
- [18] J. Plebanski, "Filtering antennas and filter-valve circuits," *Proc. Inst. Radio Eng.*, vol. 17, no. 1, pp. 161–173, Jan. 1929, doi: [10.1109/JRPROC.1929.221566](https://doi.org/10.1109/JRPROC.1929.221566).
- [19] C.-L. Ren and H.-C. Wang, "2 GHz feed for horn-reflector antenna utilizing evanescent mode filter," in *IEEE MTT-S Int. Microw. Symp. Dig.*, Jan. 1977, pp. 545–546.
- [20] D. Sanchez-Hernandez and I. Robertson, "Dual-band microstrip rectangular patch antenna using a spur-line filter technique," in *Proc. 23rd Eur. Microw. Conf.*, Oct. 1993, pp. 357–360.
- [21] A. Abbaspour-Tamijani, J. Rizk, and G. Rebeiz, "Integration of filters and microstrip antennas," in *Proc. IEEE Antennas Propag. Soc. Int. Symp.*, Feb. 2002, pp. 874–877.
- [22] F. Queudet, B. Froppier, Y. Mahe, and S. Toutain, "Study of a leaky waveguide for the design of filtering antennas," in *Proc. 33rd Eur. Microw. Conf.*, Oct. 2003, pp. 943–946.
- [23] X. Xu, M. Zhang, J. Hirokawa, and M. Ando, "E-band plate-laminated waveguide filters and their integration into a corporate-feed slot array antenna with diffusion bonding technology," *IEEE Trans. Microw. Theory Techn.*, vol. 64, no. 11, pp. 3592–3603, Nov. 2016, doi: [10.1109/TMTT.2016.2602859](https://doi.org/10.1109/TMTT.2016.2602859).
- [24] W. Wang, Z. Zheng, X. Fang, H. Zhang, M. Jin, J. Lu, Q. Luo, and S. Gao, "A waveguide slot filtering antenna with an embedded metamaterial structure," *IEEE Trans. Antennas Propag.*, vol. 67, no. 5, pp. 2953–2960, May 2019, doi: [10.1109/TAP.2019.2898989](https://doi.org/10.1109/TAP.2019.2898989).
- [25] K.-R. Xiang, F.-C. Chen, and Q.-X. Chu, "A tunable filtering antenna based on coaxial cavity resonators," *IEEE Trans. Antennas Propag.*, vol. 70, no. 5, pp. 3259–3268, May 2022, doi: [10.1109/TAP.2021.3137516](https://doi.org/10.1109/TAP.2021.3137516).
- [26] Z. Zheng, W. Wang, H.-T. Zhang, Y.-Y. Zheng, and X.-L. Liang, "Dual-band anti-interference slot antenna using metamaterial structure," in *Proc. IEEE Int. Symp. Antennas Propag. USNC-URSI Radio Sci. Meeting*, Jul. 2019, pp. 327–328.
- [27] Z. Zheng, X. Fang, W. Wang, G. Huang, H. Zhang, and X. Liang, "A compact waveguide slot filtering antenna based on mushroom-type surface," *IEEE Antennas Wireless Propag. Lett.*, vol. 19, no. 10, pp. 1823–1827, Oct. 2020, doi: [10.1109/LAWP.2020.3020539](https://doi.org/10.1109/LAWP.2020.3020539).
- [28] T. Stander and P. Meyer, "Etched ring absorbing waveguide filter based on a slotted waveguide antenna response," *Microw. Opt. Technol. Lett.*, vol. 50, no. 4, pp. 977–981, Apr. 2008, doi: [10.1002/MOP.23262](https://doi.org/10.1002/MOP.23262).

- [29] Z. Hu, S. Wang, H. Tu, Y. Li, Y. Yu, and D. Wu, "Coaxial probe-fed open-ended waveguide antenna based on sand casting process with filtering characteristics and all-in-one structure," *Int. J. RF Microw. Comput.-Aided Eng.*, vol. 31, no. 1, Jan. 2021, Art. no. e22494, doi: [10.1002/MMCE.22494](https://doi.org/10.1002/MMCE.22494).
- [30] Y. Yu, S. Wang, W. Ge, F. Zhang, G. Zhang, Y. Li, and S. Wong, "Fully integrated design of a probe-fed open-ended waveguide filtering antenna using 3-D printing technology," *Int. J. RF Microw. Comput.-Aided Eng.*, vol. 31, no. 7, Jul. 2021, Art. no. e22680, doi: [10.1002/MMCE.22680](https://doi.org/10.1002/MMCE.22680).
- [31] J. Rao, K. Nai, P. Vaitukitis, and J. Hong, "3-D metal printed high-Q folded waveguide filter with folded antenna," in *Proc. IEEE Asia-Pacific Microw. Conf. (APMC)*, Dec. 2020, pp. 619–621.
- [32] C. S. Cabello and E. Rajo-Iglesias, "Low cost self-diplexed antenna in inverted microstrip gap waveguide technology," in *Proc. Int. Symp. Antennas Propag. Conf.*, Dec. 2014, pp. 169–170.
- [33] T.-Y. Huang, H.-W. Chou, and W.-H. Hsiao, "A polarization reconfigurable microstrip circular patch filtering antenna," in *Proc. IEEE Asia-Pacific Microw. Conf. (APMC)*, Dec. 2019, pp. 1191–1193.
- [34] Z. Chen, X. Dai, and G. Luo, "A new H-slot coupled microstrip filter-antenna for modern wireless communication systems," in *Proc. Int. Workshop Antenna Technol. (iWAT)*, Mar. 2018, pp. 1–3.
- [35] W.-J. Wu, R. Fan, J. Wang, and Q. Zhang, "A broadband low profile microstrip filter-antenna with an omni-directional pattern," in *Proc. 3rd Asia-Pacific Conf. Antennas Propag.*, Jul. 2014, pp. 580–582.
- [36] Z. Zheng, D. Li, X. Tan, Y. Liu, Z. Chen, and Y. Deng, "A new differential dual-polarized filtering microstrip patch antenna without extra circuit," in *Proc. IEEE 4th Int. Conf. Electron. Inf. Commun. Technol. (ICEICT)*, Aug. 2021, pp. 750–752.
- [37] F. Xu and K. Wu, "Guided-wave and leakage characteristics of substrate integrated waveguide," *IEEE Trans. Microw. Theory Techn.*, vol. 53, no. 1, pp. 66–73, Jan. 2005, doi: [10.1109/TMTT.2004.839303](https://doi.org/10.1109/TMTT.2004.839303).
- [38] D. Deslandes and K. Wu, "Accurate modeling, wave mechanisms, and design considerations of a substrate integrated waveguide," *IEEE Trans. Microw. Theory Techn.*, vol. 54, no. 6, pp. 2516–2526, Jun. 2006, doi: [10.1109/TMTT.2006.875807](https://doi.org/10.1109/TMTT.2006.875807).
- [39] L. Wu, "Substrate integrated waveguide antenna applications," Ph.D. dissertation, School Eng. Digit. Arts, Univ. Kent, Canterbury, U.K., 2015. [Online]. Available: <https://kar.kent.ac.uk/50526/>
- [40] Y. Ding and K. Wu, "Miniaturized hybrid ring circuits using T-type folded substrate integrated waveguide (TFSIW)," in *IEEE MTT-S Int. Microw. Symp. Dig.*, Jun. 2009, pp. 705–708.
- [41] C. A. Zhang, Y. J. Cheng, and Y. Fan, "Quadri-folded substrate integrated waveguide cavity and its miniaturized bandpass filter applications," *Prog. Electromagn. Res. C*, vol. 23, pp. 1–14, 2011, doi: [10.2528/PIERC11052401](https://doi.org/10.2528/PIERC11052401).
- [42] S. Moitra and P. S. Bhowmik, "Modelling and analysis of substrate integrated waveguide (SIW) and half-mode SIW (HMSIW) band-pass filter using reactive longitudinal periodic structures," *AEU Int. J. Electron. Commun.*, vol. 70, no. 12, pp. 1593–1600, Dec. 2016, doi: [10.1016/J.AEUE.2016.09.005](https://doi.org/10.1016/J.AEUE.2016.09.005).
- [43] L. Riaz, U. Naeem, and M. F. Shafique, "Miniaturization of SIW cavity filters through stub loading," *IEEE Microw. Wireless Compon. Lett.*, vol. 26, no. 12, pp. 981–983, Dec. 2016, doi: [10.1109/LMWC.2016.2623242](https://doi.org/10.1109/LMWC.2016.2623242).
- [44] L.-N. Chen, Y.-C. Jiao, Z. Zhang, and F.-S. Zhang, "Miniaturized substrate integrated waveguide dual-mode filters loaded by a series of cross-slot structures," *Prog. Electromagn. Res. C*, vol. 29, pp. 29–39, 2012, doi: [10.2528/PIERC12032302](https://doi.org/10.2528/PIERC12032302).
- [45] A. P. Saghati, A. P. Saghati, and K. Entesar, "Ultra-miniature SIW cavity resonators and filters," *IEEE Trans. Microw. Theory Techn.*, vol. 63, no. 12, pp. 4329–4340, Dec. 2015, doi: [10.1109/TMTT.2015.2494023](https://doi.org/10.1109/TMTT.2015.2494023).
- [46] A. N. Alkhafaji, A. J. Salim, and J. K. Ali, "Compact substrate integrated waveguide BPF for wideband communication applications," in *Proc. Prog. Electromagn. Res. Symp. (PIERS)*, Jul. 2015, pp. 135–139.
- [47] H. Zhang, W. Kang, and W. Wu, "Miniaturized dual-band SIW filters using E-shaped slotlines with controllable center frequencies," *IEEE Microw. Wireless Compon. Lett.*, vol. 28, no. 4, pp. 311–313, Apr. 2018, doi: [10.1109/LMWC.2018.2811251](https://doi.org/10.1109/LMWC.2018.2811251).
- [48] H. Xia and Z. Xu, "Miniaturized multilayer dual-mode substrate integrated waveguide filter with multiple transmission zeros," *Prog. Electromagn. Res.*, vol. 139, pp. 627–642, 2013, doi: [10.2528/PIER13041112](https://doi.org/10.2528/PIER13041112).
- [49] L.-N. Chen, Y.-C. Jiao, Z. Zhang, F.-S. Zhang, and Y.-Y. Chen, "Miniaturized dual-mode substrate integrated waveguide (SIW) band-pass filters loaded by double/single T-shaped structures," *Prog. Electromagn. Res. Lett.*, vol. 29, pp. 65–74, 2012, doi: [10.2528/PIERL11112602](https://doi.org/10.2528/PIERL11112602).
- [50] A. Niembro-Martín, "Slow-wave substrate integrated waveguide," *IEEE Trans. Microw. Theory Techn.*, vol. 62, no. 8, pp. 1625–1633, Aug. 2014, doi: [10.1109/TMTT.2014.2328974](https://doi.org/10.1109/TMTT.2014.2328974).
- [51] A. Parameswaran, P. Athira, and S. Raghavan, "Miniaturizing SIW filters with slow wave technique," *AEU Int. J. Electron. Commun.*, vol. 84, pp. 360–365, Feb. 2018, doi: [10.1016/J.AEUE.2017.11.021](https://doi.org/10.1016/J.AEUE.2017.11.021).
- [52] M. Bertrand, Z. Liu, E. Pistono, D. Kaddour, and P. Ferrari, "A compact slow-wave substrate integrated waveguide cavity filter," in *IEEE MTT-S Int. Microw. Symp. Dig.*, May 2015, pp. 1–3.
- [53] M. Bertrand, E. Pistono, D. Kaddour, V. Puyal, and P. Ferrari, "A filter synthesis procedure for slow wave substrate-integrated waveguide based on a distribution of blind via holes," *IEEE Trans. Microw. Theory Techn.*, vol. 66, no. 6, pp. 3019–3027, Dec. 2018, doi: [10.1109/TMTT.2018.2825403](https://doi.org/10.1109/TMTT.2018.2825403).
- [54] J. M. George and S. Raghavan, "A design of miniaturized SIW-based band-pass cavity filter," in *Proc. Int. Conf. Commun. Signal Process. (ICCCSP)*, Apr. 2017, pp. 0622–0624.
- [55] Y.-N. Yang, G. H. Li, L. Sun, W. Yang, and X. Yang, "Design of compact bandpass filters using sixteenth mode and thirty-second mode SIW cavities," *Prog. Electromagn. Res. Lett.*, vol. 75, pp. 61–66, 2018, doi: [10.2528/PIERL18021002](https://doi.org/10.2528/PIERL18021002).
- [56] A. Iqbal, J. J. Tiang, C. K. Lee, N. K. Mallat, and S. W. Wong, "Dual-band half mode substrate integrated waveguide filter with independently tunable bands," *IEEE Trans. Circuits Syst. II, Exp. Briefs*, vol. 67, no. 2, pp. 285–289, Feb. 2020, doi: [10.1109/TCSII.2019.2911014](https://doi.org/10.1109/TCSII.2019.2911014).
- [57] B. You, L. Chen, and G. Luo, "The novel reconfigurable double-layer half-mode SIW filter with tunable DMS structure," *J. Electromagn. Waves Appl.*, vol. 32, no. 14, pp. 1816–1823, Sep. 2018, doi: [10.1080/09205071.2018.1476183](https://doi.org/10.1080/09205071.2018.1476183).
- [58] X. Nie and W. Hong, "Miniaturized QMSIW filter using comb line with high out-of-band rejection," *Electron. Lett.*, vol. 53, no. 12, pp. 785–787, Jun. 2017, doi: [10.1049/EL.2017.0899](https://doi.org/10.1049/EL.2017.0899).
- [59] Y.-D. Wu, G. H. Li, W. Yang, and X. Yang, "Design of compact wideband QMSIW band-pass filter with improved stopband," *Prog. Electromagn. Res. Lett.*, vol. 65, pp. 75–79, 2017, doi: [10.2528/PIERL16110301](https://doi.org/10.2528/PIERL16110301).
- [60] L. Li, Z. Wu, K. Yang, X. Lai, and Z. Lei, "A novel miniature single-layer eighth-mode SIW filter with improved Out-of-Band rejection," *IEEE Microw. Wireless Compon. Lett.*, vol. 28, no. 5, pp. 407–409, May 2018, doi: [10.1109/LMWC.2018.2813883](https://doi.org/10.1109/LMWC.2018.2813883).
- [61] Q. Liu, D. Zhou, D. Zhang, C. Bian, and Y. Zhang, "Ultra-compact quasi-elliptic bandpass filter based on capacitive-loaded eighth-mode SIW cavities," *Int. J. Microw. Wireless Technol.*, vol. 12, no. 2, pp. 109–115, Mar. 2020, doi: [10.1017/S175907871900120X](https://doi.org/10.1017/S175907871900120X).
- [62] A. R. Azad and A. Mohan, "A compact sixteenth-mode substrate integrated waveguide bandpass filter with improved out-of-band performance," *Microw. Opt. Technol. Lett.*, vol. 59, no. 7, pp. 1728–1733, Jul. 2017, doi: [10.1002/MOP.30615](https://doi.org/10.1002/MOP.30615).
- [63] P. Chen, X. Liu, L. Li, and K. Yang, "Miniaturized sixteenth-mode substrate integrated waveguide bandpass filter with helical slot lines," in *Proc. IEEE Asia-Pacific Microw. Conf. (APMC)*, Dec. 2019, pp. 1137–1139.
- [64] A. R. Azad and A. Mohan, "Sixteenth-mode substrate integrated waveguide bandpass filter loaded with complementary split-ring resonator," *Electron. Lett.*, vol. 53, no. 8, pp. 546–547, Apr. 2017, doi: [10.1049/EL.2016.3620](https://doi.org/10.1049/EL.2016.3620).
- [65] G. Q. Luo, "Filter antenna consisting of horn antenna and substrate integrated waveguide cavity FSS," *IEEE Trans. Antennas Propag.*, vol. 55, no. 1, pp. 92–98, Jan. 2007, doi: [10.1109/TAP.2006.888459](https://doi.org/10.1109/TAP.2006.888459).
- [66] O. A. Nova, J. C. Bohorquez, and N. M. Pena, "An approach to filter-antenna integration in SIW technology," in *Proc. IEEE 2nd Latin Amer. Symp. Circuits Syst. (LASCAS)*, Feb. 2011, pp. 1–4.
- [67] Y. Chen, W. Hong, Z. Kuai, and H. Wang, "Ku-band linearly polarized omnidirectional planar filter antenna," *IEEE Antennas Wireless Propag. Lett.*, vol. 11, pp. 310–313, Mar. 2012, doi: [10.1109/LAWP.2012.2191259](https://doi.org/10.1109/LAWP.2012.2191259).
- [68] Z. Xue, Y. Zhang, and W. Hong, "Design and implementation of a filter antenna with wide beamwidth for Q-Band millimeter-wave short range wireless communications," in *Proc. Int. Symp. Antennas, Propag.*, Jan. 2013, pp. 909–912.

- [69] K.-Z. Hu, M.-C. Tang, M. Li, and R. W. Ziolkowski, "Compact, low-profile, bandwidth-enhanced substrate integrated waveguide filterna," *IEEE Antennas Wireless Propag. Lett.*, vol. 17, no. 8, pp. 1552–1556, Aug. 2018, doi: [10.1109/LAWP.2018.2854898](https://doi.org/10.1109/LAWP.2018.2854898).
- [70] H. Cheng, Y. Yusuf, and X. Gong, "Vertically integrated three-pole filter/antennas for array applications," *IEEE Antennas Wireless Propag. Lett.*, vol. 10, pp. 278–281, 2011, doi: [10.1109/LAWP.2011.2135833](https://doi.org/10.1109/LAWP.2011.2135833).
- [71] Y. Yusuf, H. Cheng, and X. Gong, "A seamless integration of 3-D vertical filters with highly efficient slot antennas," *IEEE Trans. Antennas Propag.*, vol. 59, no. 11, pp. 4016–4022, Nov. 2011, doi: [10.1109/TAP.2011.2164186](https://doi.org/10.1109/TAP.2011.2164186).
- [72] Y. Zhang, X. Y. Zhang, and Q. H. Liu, "A dual-layer filtering SIW slot antenna utilizing double slot coupling scheme," *IEEE Antennas Wireless Propag. Lett.*, vol. 20, no. 6, pp. 1073–1077, Jun. 2021, doi: [10.1109/LAWP.2021.3071528](https://doi.org/10.1109/LAWP.2021.3071528).
- [73] C. X. Mao, L. Zhang, M. Khalily, Y. Gao, and P. Xiao, "A multiplexing filtering antenna," *IEEE Trans. Antennas Propag.*, vol. 69, no. 8, pp. 5066–5071, Aug. 2021, doi: [10.1109/TAP.2020.3048589](https://doi.org/10.1109/TAP.2020.3048589).
- [74] H. Chu, J.-X. Chen, S. Luo, and Y.-X. Guo, "A millimeter-wave filtering monopulse antenna array based on substrate integrated waveguide technology," *IEEE Trans. Antennas Propag.*, vol. 64, no. 1, pp. 316–321, Jan. 2016, doi: [10.1109/TAP.2015.2497351](https://doi.org/10.1109/TAP.2015.2497351).
- [75] H. Chu and Y.-X. Guo, "A filtering dual-polarized antenna subarray targeting for base stations in millimeter-wave 5G wireless communications," *IEEE Trans. Compon., Packag., Manuf. Technol.*, vol. 7, no. 6, pp. 964–973, May 2017, doi: [10.1109/TCPM.2017.2694848](https://doi.org/10.1109/TCPM.2017.2694848).
- [76] T. Li and X. Gong, "Vertical integration of high-Q filter with circularly polarized patch antenna with enhanced impedance-axial ratio bandwidth," *IEEE Trans. Antennas Propag.*, vol. 66, no. 6, pp. 3119–3128, Jun. 2018, doi: [10.1109/TMTT.2018.2832073](https://doi.org/10.1109/TMTT.2018.2832073).
- [77] M.-M. Yang, L. Zhang, Y. Zhang, H.-W. Yu, and Y.-C. Jiao, "Filtering antenna with quasi-elliptic response based on SIW H-Plane horn," *IEEE Antennas Wireless Propag. Lett.*, vol. 20, no. 7, pp. 1302–1306, Jul. 2021, doi: [10.1109/LAWP.2021.3078535](https://doi.org/10.1109/LAWP.2021.3078535).
- [78] L. Liu, T.-L. Bai, J.-Y. Deng, D. Sun, Y. Zhang, T. Yong, S.-G. Zhou, and L.-X. Guo, "Substrate integrated waveguide filtering horn antenna facilitated by embedded via-hole arrays," *IEEE Antennas Wireless Propag. Lett.*, vol. 19, no. 7, pp. 1187–1191, Jul. 2020, doi: [10.1109/LAWP.2020.2994617](https://doi.org/10.1109/LAWP.2020.2994617).
- [79] Z. Wang and Y. Dong, "Circularly polarized antennas inspired by dual-mode SIW cavities," *IEEE Access*, vol. 7, pp. 173007–173018, 2019, doi: [10.1109/ACCESS.2019.2956750](https://doi.org/10.1109/ACCESS.2019.2956750).
- [80] Z. Wang and Y. Dong, "Development of low-profile filtering antennas with dual-mode cavities," *IEEE Open J. Antennas Propag.*, vol. 1, pp. 159–164, 2020, doi: [10.1109/OJAP.2020.2988569](https://doi.org/10.1109/OJAP.2020.2988569).
- [81] X. Liu, X. Zhang, K. Xu, and J. Shi, "A filtering antenna with high frequency selectivity using stacked dual-slotted substrate integrated cavities," *IEEE Antennas Wireless Propag. Lett.*, vol. 19, no. 8, pp. 1311–1315, Aug. 2020, doi: [10.1109/LAWP.2020.2998125](https://doi.org/10.1109/LAWP.2020.2998125).
- [82] H.-Y. Xie, B. Wu, Y.-L. Wang, C. Fan, J.-Z. Chen, and T. Su, "Wideband SIW filtering antenna with controllable radiation nulls using dual-mode cavities," *IEEE Antennas Wireless Propag. Lett.*, vol. 20, no. 9, pp. 1799–1803, Sep. 2021, doi: [10.1109/LAWP.2021.3097214](https://doi.org/10.1109/LAWP.2021.3097214).
- [83] D. Zhao, F. Lin, H. Sun, and X. Y. Zhang, "A miniaturized dual-band SIW filtering antenna with improved out-of-band suppression," *IEEE Trans. Antennas Propag.*, vol. 70, no. 1, pp. 126–134, Jan. 2022, doi: [10.1109/TAP.2021.3098561](https://doi.org/10.1109/TAP.2021.3098561).
- [84] S. Cai, J. Liu, and Y. Long, "Investigation of SIW cavity-backed slot and patch antennas with conical radiation patterns," *IEEE Trans. Antennas Propag.*, vol. 68, no. 8, pp. 5978–5988, Aug. 2020, doi: [10.1109/TAP.2020.2990312](https://doi.org/10.1109/TAP.2020.2990312).
- [85] S. Ji, Y. Dong, Y. Pan, Y. Zhu, and Y. Fan, "Planar circularly polarized antenna with bandpass filtering response based on dual-mode SIW cavity," *IEEE Trans. Antennas Propag.*, vol. 69, no. 6, pp. 3155–3164, Jun. 2021, doi: [10.1109/TAP.2020.3037819](https://doi.org/10.1109/TAP.2020.3037819).
- [86] Y. Shi, J. Liu, and Y. Long, "Wideband triple- and quad-resonance substrate integrated waveguide cavity-backed slot antennas with shorting vias," *IEEE Trans. Antennas Propag.*, vol. 65, no. 11, pp. 5768–5775, Nov. 2017, doi: [10.1109/TAP.2017.2755118](https://doi.org/10.1109/TAP.2017.2755118).
- [87] Y. Feng, S. Fang, S. Jia, and Z. Xu, "Tri-layered stacked substrate integrated waveguide bandpass filter using non-resonant nodes excitation," *IEEE Trans. Circuits Syst. II, Exp. Briefs*, vol. 69, no. 3, pp. 1004–1008, Mar. 2022, doi: [10.1109/TCSII.2021.3122254](https://doi.org/10.1109/TCSII.2021.3122254).
- [88] Y. Feng, S. Fang, L. Zhou, Q. Zhang, and Z. Xu, "Compact triple-mode bandpass filters based on single perturbed substrate integrated waveguide cavity using coaxial feed," *Microw. Opt. Technol. Lett.*, vol. 64, no. 2, pp. 223–230, Feb. 2022, doi: [10.1002/MOP.33073](https://doi.org/10.1002/MOP.33073).
- [89] P. K. Li, C. J. You, H. F. Yu, X. Li, Y. W. Yang, and J. H. Deng, "Codesigned high-efficiency single-layered substrate integrated waveguide filtering antenna with a controllable radiation null," *IEEE Antennas Wireless Propag. Lett.*, vol. 17, no. 2, pp. 295–298, Feb. 2018, doi: [10.1109/LAWP.2017.2787541](https://doi.org/10.1109/LAWP.2017.2787541).
- [90] K.-Z. Hu, M.-C. Tang, Y. Wang, D. Li, and M. Li, "Compact, vertically integrated duplex filterna with common feeding and radiating SIW cavities," *IEEE Trans. Antennas Propag.*, vol. 69, no. 1, pp. 502–507, Jan. 2021, doi: [10.1109/TAP.2020.2999381](https://doi.org/10.1109/TAP.2020.2999381).
- [91] A. Kumar and A. A. Althuwayb, "SIW resonator-based duplex filterna," *IEEE Antennas Wireless Propag. Lett.*, vol. 20, no. 12, pp. 2544–2548, Dec. 2021, doi: [10.1109/LAWP.2021.3118566](https://doi.org/10.1109/LAWP.2021.3118566).
- [92] B. Niu and J. Tan, "Low-profile SIW cavity antenna with enhanced bandwidth and controllable radiation null," *Microw. Opt. Technol. Lett.*, vol. 62, no. 5, pp. 2014–2018, May 2020, doi: [10.1002/mop.32249](https://doi.org/10.1002/mop.32249).
- [93] B. Niu, J. Tan, and S. Wong, "Compact SIW cavity slot antenna with enhanced bandwidth and quasi-elliptic filtering response," *Electron. Lett.*, vol. 55, no. 2, pp. 69–70, Jan. 2019, doi: [10.1049/EL.2018.7619](https://doi.org/10.1049/EL.2018.7619).
- [94] C. Fan, B. Wu, Y.-L. Wang, H.-Y. Xie, and T. Su, "High-gain SIW filtering antenna with low H-plane cross polarization and controllable radiation nulls," *IEEE Trans. Antennas Propag.*, vol. 69, no. 4, pp. 2336–2340, Apr. 2021, doi: [10.1109/TAP.2020.3018595](https://doi.org/10.1109/TAP.2020.3018595).
- [95] R. Lovato and X. Gong, "A third-order SIW-integrated filter/antenna using two resonant cavities," *IEEE Antennas Wireless Propag. Lett.*, vol. 17, no. 3, pp. 505–508, Mar. 2018, doi: [10.1109/LAWP.2018.2799518](https://doi.org/10.1109/LAWP.2018.2799518).
- [96] K.-Z. Hu, M.-C. Tang, D. Li, Y. Wang, and M. Li, "Design of compact, single-layered substrate integrated waveguide filterna with parasitic patch," *IEEE Trans. Antennas Propag.*, vol. 68, no. 2, pp. 1134–1139, Feb. 2020, doi: [10.1109/TAP.2019.2938574](https://doi.org/10.1109/TAP.2019.2938574).
- [97] Q. Liu, L. Zhu, J. Wang, and W. Wu, "A wideband patch and SIW cavity hybrid antenna with filtering response," *IEEE Antennas Wireless Propag. Lett.*, vol. 19, no. 5, pp. 836–840, May 2020, doi: [10.1109/LAWP.2020.2981650](https://doi.org/10.1109/LAWP.2020.2981650).
- [98] J.-Y. Yin, T.-L. Bai, J.-Y. Deng, J. Ren, D. Sun, Y. Zhang, and L.-X. Guo, "Wideband single-layer substrate integrated waveguide filtering antenna with U-shaped slots," *IEEE Antennas Wireless Propag. Lett.*, vol. 20, no. 9, pp. 1726–1730, Sep. 2021, doi: [10.1109/LAWP.2021.3095188](https://doi.org/10.1109/LAWP.2021.3095188).
- [99] C. Wang, X. Wang, H. Liu, Z. Chen, and Z. Han, "Substrate integrated waveguide filterna with two controllable radiation nulls," *IEEE Access*, vol. 8, pp. 120019–120024, 2020, doi: [10.1109/ACCESS.2020.3005948](https://doi.org/10.1109/ACCESS.2020.3005948).
- [100] S. Yu, F. Cheng, C. Gu, B. Zhang, and K. Huang, "Substrate integrated waveguide omnidirectional filtering antenna with a controllable radiation null for 5.8 GHz WiFi application," *Int. J. RF Microw. Comput.-Aided Eng.*, vol. 32, no. 3, Mar. 2022, Art. no. e23007, doi: [10.1002/MMCE.23007](https://doi.org/10.1002/MMCE.23007).
- [101] H. Liu, T. Liu, Q. Zhang, B. Ren, and P. Wen, "Compact balanced bandpass filter design using asymmetric SIR pairs and spoof surface plasmon polariton feeding structure," *IEEE Microw. Wireless Compon. Lett.*, vol. 28, no. 11, pp. 987–989, Nov. 2018, doi: [10.1109/LMWC.2018.2873209](https://doi.org/10.1109/LMWC.2018.2873209).
- [102] Z. Sakotic, M. Drljaca, G. Kitic, N. Jankovic, and N. Cseljuszka, "LTCC dual-band bandpass filter based on SPlike propagation in substrate integrated waveguide," in *Proc. IEEE EUROCON 18th Int. Conf. Smart Technol.*, Jul. 2019, pp. 1–4.
- [103] M. Du, K. Chen, and Y. Feng, "Filtering balun based on spoof surface plasmon polariton," in *Proc. Cross Strait Quad-Regional Radio Sci. Wireless Technol. Conf. (CSQRWC)*, Jul. 2018, pp. 1–3.
- [104] J. Luo, J. He, A. Apriyana, G. Feng, Q. Huang, and Y. P. Zhang, "Tunable surface-plasmon-polariton filter constructed by corrugated metallic line and high permittivity material," *IEEE Access*, vol. 6, pp. 10358–10364, 2018, doi: [10.1109/ACCESS.2018.2800158](https://doi.org/10.1109/ACCESS.2018.2800158).
- [105] Q. L. Zhang and C. H. Chan, "Spoof surface plasmon polariton filter with reconfigurable dual and non-linear notched characteristics," *IEEE Trans. Circuits Syst. II, Exp. Briefs*, vol. 68, no. 8, pp. 2815–2819, Aug. 2021, doi: [10.1109/TCSII.2021.3067936](https://doi.org/10.1109/TCSII.2021.3067936).
- [106] Y. Gou, Z. X. Wang, L. W. Wu, and H. F. Ma, "Compact rejection filters based on the interaction between spoof SPPs and LSPs," in *Proc. Int. Conf. Microw. Millim. Wave Technol. (ICMMT)*, May 2019, pp. 1–4.

- [107] M. Hu, X. Huo, J. Liu, W. Tang, and Z. Zeng, "A band pass microwave filter with planar spoof surface plasmon polaritons structure," in *Proc. IEEE 2nd Adv. Inf. Technol., Electron. Autom. Control Conf. (IAEAC)*, Mar. 2017, pp. 2219–2222.
- [108] D.-F. Guan, P. You, Q. Zhang, K. Xiao, and S. W. Yong, "Hybrid spoof surface plasmon polariton and substrate integrated waveguide transmission line and its application in filter," *IEEE Trans. Microw. Theory Techn.*, vol. 65, no. 12, pp. 4925–4932, Dec. 2017, doi: [10.1109/TMTT.2017.2727486](https://doi.org/10.1109/TMTT.2017.2727486).
- [109] Z. Li, L. Liu, H. Sun, Y. Sun, C. Gu, X. Chen, Y. Liu, and Y. Luo, "Effective surface plasmon polaritons induced by modal dispersion in a waveguide," *Phys. Rev. A, Gen. Phys.*, vol. 7, no. 4, Apr. 2017, Art. no. 044028, doi: [10.1103/PhysRevApplied.7.044028](https://doi.org/10.1103/PhysRevApplied.7.044028).
- [110] N. Cselyuska, Z. Sakotic, G. Kitic, V. Crnojevic-Bengin, and N. Jankovic, "Novel dual-band band-pass filters based on surface plasmon polariton-like propagation induced by structural dispersion of substrate integrated waveguide," *Sci. Rep.*, vol. 8, no. 1, p. 8332, May 2018, doi: [10.1038/s41598-018-26705-w](https://doi.org/10.1038/s41598-018-26705-w).
- [111] X.-F. Zhang, S.-H. Cao, and J.-X. Chen, "Novel millimeter-wave bandwidth-controllable filtering antenna based on composite ESPPs-SIW structure," *IEEE Trans. Antennas Propag.*, vol. 69, no. 11, pp. 7924–7929, Nov. 2021, doi: [10.1109/TAP.2021.3088538](https://doi.org/10.1109/TAP.2021.3088538).
- [112] O. Losito, "X-band SIW cavity-backed patch antenna for radar applications," in *Proc. Eur. Microw. Conf.*, Jan. 2013, pp. 199–202.
- [113] Y. Yu, W. Hong, H. Zhang, J. Xu, and Z. H. Jiang, "Optimization and implementation of SIW slot array for both medium- and long-range 77 GHz automotive radar application," *IEEE Trans. Antennas Propag.*, vol. 66, no. 7, pp. 3769–3774, Jul. 2018, doi: [10.1109/TAP.2018.2823911](https://doi.org/10.1109/TAP.2018.2823911).
- [114] J. Xie, Q. Wu, C. Yu, H. Wang, and W. Hong, "Wideband SIW cavity-backed slot array antenna with flat gain characteristics for 79 GHz automotive radar," in *Proc. 13th Eur. Conf. Antennas, Propag. (EuCAP)*, Mar. 2019, pp. 1–4.
- [115] A. P. Saghati, A. P. Saghati, and K. Entesari, "A SIW uniform circular antenna array for 5G applications fed by a radially-symmetric eight-way SIW power divider," in *Proc. IEEE Int. Symp. Antennas Propag. USNC-URSI Radio Sci. Meeting*, Jul. 2019, pp. 1343–1344.
- [116] M. Rizal, N. Ismail, K. A. Munastha, and A. Munir, "SIW-based radial-line-slot-array antenna for wireless communication," in *Proc. 14th Int. Conf. Telecommun. Syst., Services, Appl. (TSSA)*, Nov. 2020, pp. 1–4.
- [117] P. Nuangpirom, K. Ruangsiri, and S. Akatimagoon, "Low-profile, MIMO antenna based on substrate integrated waveguide for WLAN applications," in *Proc. 16th Int. Conf. Electr. Eng./Electron., Comput., Telecommun. Inf. Technol. (ECTI-CON)*, Jul. 2019, pp. 740–743.
- [118] A. Izzuddin, A. Dewantari, E. Setijadi, E. Palantei, E. T. Rahardjo, and A. Munir, "Design of 2.4 GHz slotted SIW array antenna for WLAN application," in *Proc. Int. Conf. Radar, Antenna, Microw., Electron., Telecommun. (ICRAMET)*, Nov. 2020, pp. 70–73.
- [119] Z. Xu, J. Shi, R. J. Davis, X. Yin, and D. F. Sievenpiper, "Rainbow trapping with long oscillation lifetimes in gradient magnetoinductive metasurfaces," *Phys. Rev. A, Gen. Phys.*, vol. 12, no. 2, Aug. 2019, Art. no. 024043, doi: [10.1103/PhysRevApplied.12.024043](https://doi.org/10.1103/PhysRevApplied.12.024043).
- [120] P. Zhou, H. Zhao, Z. Xu, S. Li, Y. Shi, and X. Yin, "Analysis and modeling of wideband common-mode absorption with lossy complementary splitting resonator chain in resistor-free differential microstrip lines," *IEEE Trans. Microw. Theory Techn.*, vol. 70, no. 2, pp. 1048–1058, Feb. 2022, doi: [10.1109/TMTT.2021.3126879](https://doi.org/10.1109/TMTT.2021.3126879).



XIAONAN SUN was born in Jilin, China. She received the B.E. degree in electronic information science and technology from Dalian Maritime University, Dalian, China, in 2021, where she is currently pursuing the master's degree. Her research interests include microwave circuits and antennas.



JITONG MA received the B.S. degree in electronic information engineering from Hohai University, China, in 2013, the M.S. degree from the Dalian University of Technology, Dalian, China, in 2015, and the Ph.D. degree in signal and information processing from the Dalian University of Technology, in 2020. From 2018 to 2019, he was a Joint Supervision Ph.D. Student at the Department of Electrical and Computer Engineering, North Carolina State University, Raleigh, NC, USA. He is currently a Lecturer with the Information Science and Technology College, Dalian Maritime University, Dalian. His research interests include wireless communication and statistical signal processing.



YULIN FENG was born in Liaoning, China. He received the B.E. degree in electronic and information engineering from Shenyang Aerospace University (SAU), Shenyang, China, in 2019. He is currently pursuing the master's degree. His current research interests include microwave circuits and filters.



JUN SHI (Member, IEEE) was born in Jiangsu, China, in 1988. He received the B.S. degree in information engineering and the Ph.D. degree in electromagnetic field and microwave technology from Southeast University, in 2011 and 2018, respectively. His Ph.D. dissertation was in the area of wideband feed technology and cryogenic receiver design technique applied to radio astronomy. He was a Joint Ph.D. Student at Shanghai Astronomical Observatory from 2013 to 2015. He was a Visiting Student Researcher with the Department of Electrical Engineering, Caltech, from 2015 to 2016. Since 2018, he has been a Postdoctoral Scholar with the Microwave Research Group, Department of Astronomy, California Institute of Technology, Pasadena, CA, USA. His current research interests include decade bandwidth antennas, ultra-low noise amplifiers, microwave circuit components, and RF systems.



ZHIXIA XU (Member, IEEE) was born in Wuxi, China. He received the B.Eng. degree in electronic information science and technology from Dalian Maritime University, Dalian, China, in 2015, and the Ph.D. degree in electromagnetic field and microwave technique from Southeast University, Nanjing, China, in 2019. From 2018 to 2019, he was a Visiting Graduate Student at the University of California, San Diego, CA, USA. He is currently an Associate Professor with Dalian Maritime University, and he also holds a postdoctoral position with the State Key Laboratory of Millimeter Waves of Southeast University. His current research interests include periodic structures, photonic topological insulators, sensors, and antennas.